Exciton optics, dynamics, and transport in atomically thin semiconductors

APL Materials

Exciton optics, dynamics, and transport in atomically thin semiconductors

Cite as: APL Mater. **10**, 100701 (2022); https://doi.org/10.1063/5.0107665
Submitted: 06 July 2022 • Accepted: 19 September 2022 • Published Online: 31 October 2022

Raul Perea-Causin, Daniel Erkensten, Jamie M. Fitzgerald, et al.

Exciton optics, dynamics, and transport in atomically thin semiconductors

Cite as: APL Mater. 10, 100701 (2022); doi: 10.1063/5.0107665
Submitted: 6 July 2022 • Accepted: 19 September 2022 •
Published Online: 31 October 2022

Raul Perea-Causin,[1,a] Daniel Erkensten,[1,a] Jamie M. Fitzgerald,[2] Joshua J. P. Thompson,[2] Roberto Rosati,[2] Samuel Brem,[2] and Ermin Malic[1,2]

AFFILIATIONS

[1] Department of Physics, Chalmers University of Technology, 412 96 Gothenburg, Sweden
[2] Department of Physics, Philipps-Universität Marburg, 35032 Marburg, Germany

[a] Author to whom correspondence should be addressed: causin@chalmers.se and daniel.erkensten@chalmers.se

ABSTRACT

Atomically thin semiconductors such as transition metal dichalcogenide (TMD) monolayers exhibit a very strong Coulomb interaction, giving rise to a rich exciton landscape. This makes these materials highly attractive for efficient and tunable optoelectronic devices. In this Research Update, we review the recent progress in the understanding of exciton optics, dynamics, and transport, which crucially govern the operation of TMD-based devices. We highlight the impact of hexagonal boron nitride-encapsulation, which reveals a plethora of many-particle states in optical spectra, and we outline the most novel breakthroughs in the field of exciton-polaritonics. Moreover, we underline the direct observation of exciton formation and thermalization in TMD monolayers and heterostructures in recent time-resolved, angle-resolved photoemission spectroscopy studies. We also show the impact of exciton density, strain, and dielectric environment on exciton diffusion and funneling. Finally, we put forward relevant research directions in the field of atomically thin semiconductors for the near future.

I. INTRODUCTION

Atomically thin semiconductors have emerged in the last decade as a platform for investigating quantum many-body phenomena and as promising candidates for novel optoelectronic applications.[1–6] In particular, monolayers of semiconducting transition metal dichalcogenides (TMDs), including the extensively studied MoS_2, $MoSe_2$, WS_2, and WSe_2, display weak dielectric screening due to their truly two-dimensional character. Concretely, the electric field lines between two charge carriers confined in the TMD monolayer extend largely outside the material into the surrounding dielectrics, which generally possess a small permittivity. The resulting strong Coulomb interaction gives rise to rich exciton physics in TMD monolayers. Excitons, i.e., tightly bound electron–hole pairs, dominate the optical response in these materials and show large binding energies and oscillator strengths.[7]

The multi-valley band structure and sizable spin–orbit coupling in TMDs result in an abundance of optically active (bright) and inactive (dark) exciton states with different spin–valley configurations.[1,8,9] Taking advantage of their two-dimensional character, TMD monolayers can be vertically stacked to form van der Waals (vdW) heterostructures, which allows for the creation of complex materials with designed functionalities and opens up a new venue for exploring intriguing many-body physics. In particular, the exciton landscape is extended to interlayer excitons, where the constituent electrons and holes are spatially separated, i.e., they are localized in different TMD layers.[3,5,6,10] While excitons dominate the optical response in TMD monolayers and heterostructures at low or moderate carrier densities, higher-order many-particle complexes, including trions, biexcitons, and polaritons become crucial in different technologically relevant regimes, i.e., in the presence of doping, at high excitation densities, and in optical cavities, respectively.

In order to design efficient and tunable optoelectronic devices based on TMDs, the fundamental processes governing the device operation must be well understood. These processes can be grouped into three categories—optics, dynamics, and transport—which include (i) optical absorption and emission processes, (ii) exciton formation, thermalization and recombination dynamics, and (iii) exciton diffusion and funneling (cf. Fig. 1). In this Research

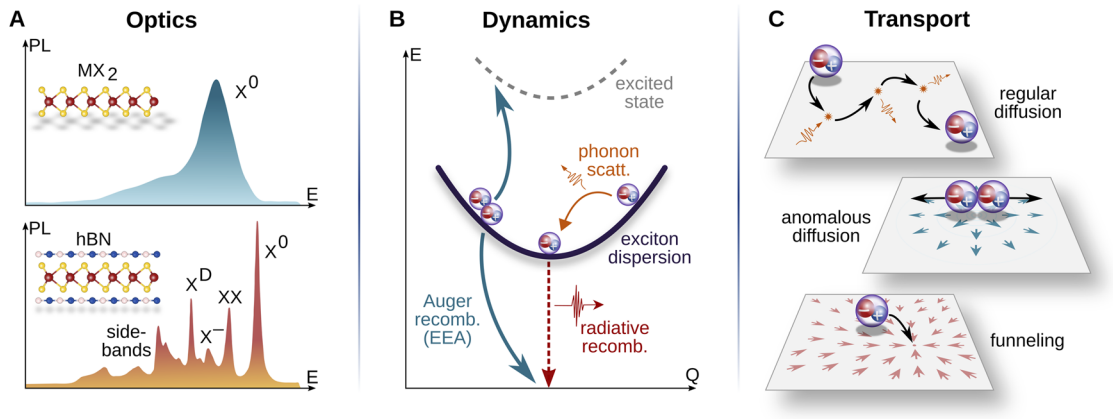

FIG. 1. Schematic illustration of the three focus areas of the review. (a) Exciton optics with a multitude of resonances in PL spectra of hBN-encapsulated TMDs, including signatures of neutral (X^0) and dark (X^D) excitons, as well as trions (X^-) and biexcitons (XX). (b) Exciton dynamics illustrating thermalization via exciton–phonon scattering and recombination via Auger scattering (exciton–exciton annihilation) and radiative channels. (c) Exciton transport including regular diffusion—dominated by exciton–phonon scattering, anomalous diffusion—governed by exciton–exciton repulsion, and exciton funneling, where the arrows in the plane illustrate the direction of the drift current.

Update, we review the recent developments in the understanding of exciton optics, dynamics, and transport in semiconducting TMD monolayers and heterostructures. In particular, we focus on the four most studied TMDs, i.e., MoS_2, $MoSe_2$, WS_2, and WSe_2. In Sec. II, we describe optical signatures of excitons and highlight the crucial impact of hexagonal boron nitride (hBN)-encapsulation, which reveals the fine structure of optical spectra with a multitude of many-particle states [cf. Fig. 1(a)]. Furthermore, we review the recent advances in the extensive field of exciton–polaritons in monolayer TMDs and heterostructures. In Sec. III, we discuss the progress in exciton dynamics including exciton formation, thermalization, and recombination [cf. Fig. 1(b)]. Here, the focus lies on the direct observation of momentum-dark excitons in time-resolved, angle-resolved photoemission spectroscopy (ARPES) measurements as well as interlayer exciton formation and recombination of moiré excitons. In Sec. IV, we summarize the recent developments in exciton transport, emphasizing the impact of exciton density, strain, and dielectric environment on exciton diffusion and funneling [cf. Fig. 1(c)]. Finally, we highlight the most promising avenues and pressing challenges for prospective research in this field.

II. EXCITON OPTICS

The close relationship between optics and excitonics represents the primary and most versatile avenue for probing and manipulating excitons in transition metal dichalcogenides.[1,2] Excitons in semiconducting TMDs are typically generated via optical excitation,[11,12] where an incident photon leads to the generation of a Coulomb-bound electron–hole pair, forming an exciton. In this section, we discuss recent advances in exciton optics, which have been enabled by hBN-encapsulation of TMD samples. The sharp spectral lines resulting from the hBN-encapsulation allowed revealing a rich excitonic substructure of bright and dark excitons, as well as higher-order charge complexes, such as trions and biexcitons. Besides the exciton physics in TMD monolayers, we also outline how optics can be used to probe the nature of excitons in TMD-based heterostructures. Furthermore, we explore how the exciton–light coupling can be enhanced by structuring the surrounding dielectric medium, e.g., in cavities, leading to the formation of exciton–polaritons.

A. Bright and dark exciton signatures

As the research field of TMDs has grown, fabrication and device design has steadily improved, with modern device architectures being of exceptionally high quality. This has been, in part, achieved through the encapsulation of TMDs with hexagonal boron nitride, an inert, two-dimensional, wide bandgap insulator. The hBN efficiently protects the TMD from typically used substrates, which generally possess many defects, dangling bonds, and a rough surface that creates dielectric inhomogeneities.[13–15] Therefore, hBN-encapsulated samples are better protected from disorder effects, which hamper the generation and detection of charge complexes.[16] This has triggered the optical detection of various excitonic and higher-order charge complex features in recent studies. In the following we will discuss signatures of bright and dark excitons which have been revealed through the improved quality of sample structures.

Absorption measurements on TMDs can directly probe the energy of optically active excitons.[17] In addition to the spectrally lowest 1s exciton, higher-order s-states,[18] as well as signatures from the optically dark p-states,[19] can be observed. Moreover, the spectral broadening of absorption resonances directly reflects both radiative and non-radiative dephasing processes.[20–26] Another important control parameter in absorption experiments is the optical polarization of the incident light. In TMDs, optical excitation by left- and right-handed circularly polarized light generates excitons at the K and K′ valleys in the electronic dispersion, respectively.[17,26–29] This

has important implications for both valleytronics[29,30] and, due to the spin–valley locking in TMDs,[32] spintronics applications.[32–35]

Excitons possess a finite lifetime[36] before undergoing radiative decay and emitting a photon. Between their creation and annihilation, however, phonon- or Coulomb-mediated scattering processes allow the generated excitons to relax into some new distribution.[37,38] By measuring the optical response from the radiative recombination of these excitons in photoluminescence (PL) experiments, it is possible to uncover additional information on excitonic processes in the TMD. In particular, PL spectra can exhibit unique signatures from the indirect recombination of dark excitons.[39,41,41] Tungsten-based TMDs (such as WS_2 and WSe_2) possess energetically lower-lying momentum-dark exciton states [cf. Fig. 2(a)], comprised of an electron and hole in different valleys in the Brillouin zone.[9,20,42] The large center-of-mass momentum of these excitons forbids direct radiative recombination. However, by simultaneous interaction with a phonon, momentum conservation can be fulfilled and the dark exciton can indirectly emit a photon, leaving behind a clear signal in the PL spectra. This process is known as phonon-assisted photoluminescence[39,40,43–45] and results in the formation of phonon sidebands, cf. Fig. 2(a). The probability of this higher-order process is significantly lower than the direct emission from a bright exciton. However, at sufficiently low temperatures, the energetically lowest dark excitons carry almost the entire population, which compensates for the much lower emission probability and results in a strong signal in the PL. Thus, in molybdenum-based TMDs, whose momentum-dark states are located higher in energy, no phonon sidebands are observed. The temperature-dependent PL spectrum for monolayer WSe_2[39] is shown in Fig. 2(b), where at high temperatures, only emission from the bright exciton can be seen. In contrast, at temperatures below 50 K, the indirect emission from dark excitons dominates the PL. Since, here, the emission of a phonon is involved, the phonon sidebands are red-shifted in energy with respect to the position of dark excitons (dashed white lines). Multiple resonances are observed due to different optical and acoustic phonons involved in this process. These phonon sidebands have been observed both for dark excitons,[39,45–47] where they dominate the PL spectra, and bright excitons, where they are hidden in an asymmetric broadening of the spectral linewidth.[39,48]

Note that besides the momentum-dark excitons discussed so far, there exist also spin-dark excitons consisting of an electron and hole with an opposite spin. These excitons can be brightened under the application of an external magnetic field[50–51] or by changing the angle of the detector/polarization.[52] In the latter case, the magnetic component of the electromagnetic field points out-of-plane and hence couples the opposite spins, allowing for the two charge carriers to recombine.

Excitons are characterized by a band structure with an effective mass determined by the excitonic center-of-mass motion [cf. Fig. 2(a)]. PL and absorption spectroscopy can only probe the small-momentum range within the light cone directly and hence do not provide any momentum-resolved information. Instead, recent studies[54–57] have employed angle-resolved photoemission

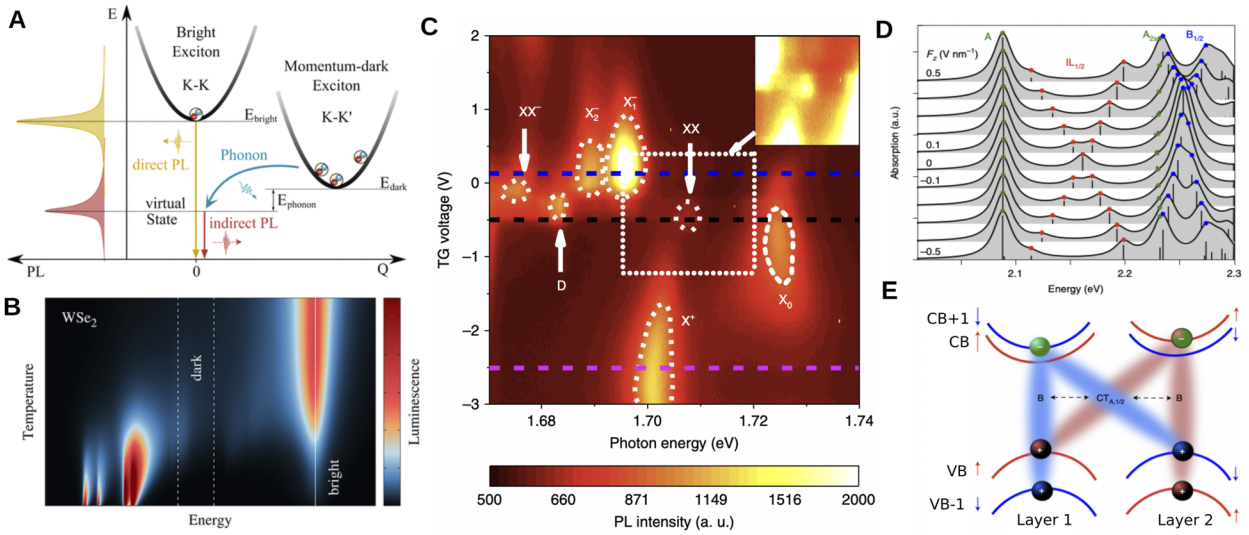

FIG. 2. Optical signatures of excitons and higher-order many-body complexes in TMD monolayers and heterostructures. (a) Sketch of the excitonic center-of-mass dispersion for a tungsten-based TMD (with energetically lower dark excitons), the direct and indirect recombination channels, and the expected PL signal. (b) Temperature-dependent PL spectrum calculated for a WSe_2 monolayer demonstrating the appearance of phonon sidebands at low temperatures. (c) PL spectrum for a hBN-encapsulated WSe_2 layer as a function of applied gate voltage, revealing a plethora of charged many-particle complexes. (d) Calculated absorption spectrum (gray shaded) and experimental peak positions (colored dots) demonstrating electric field tuning of the hybrid interlayer exciton resonance in bilayer MoS_2. (e) Schematic of the band alignment of bilayer MoS_2 at finite electric field. Panels (a) and (b) adapted with permission from Brem *et al.*, Nano Lett. **20**, 2849–2856 (2020). Copyright 2020 ACS Author(s) licensed under a Creative Commons Attribution 4.0 License; (c) adapted with permission from Li *et al.*, Nat. Commun. **9**, 3719 (2018). Copyright 2018 Springer Nature Ltd. Author(s) licensed under a Creative Commons Attribution 4.0 License; (d) and (e) adapted with permission from Peimyoo *et al.*, Nat. Nanotechnol. **16**, 888–893 (2021). Copyright 2021 Springer Nature Ltd.

spectroscopy measurements, which can be used to probe the excitonic band structure more directly. In this technique, an initial pump pulse generates excitons before a high-energy photon ejects electrons from the conduction band via the photoelectric effect. While ARPES has the advantage of resolving the electron population in the whole Brillouin zone, it is not directly clear whether the ejected conduction-band electron was bound to a hole (forming an exciton). Nevertheless, the excitonic nature of the measured signal can be determined with complementary PL or absorption spectra. Concretely, the agreement between the bandgap extracted from ARPES and the exciton resonance energy in optical spectra provides direct evidence of the excitonic nature of the ARPES signal. In Sec. III we explore how time-resolved ARPES measurements can be used to probe the exciton dynamics and, in particular, the thermalization between bright and dark excitons.[53,55]

B. Trion and biexciton signatures

The optical response of TMD monolayers is generally dominated by excitons at low and moderate excitation density in weakly doped samples. At elevated excitation densities and in the presence of doping, higher-order charge complexes become relevant. In general, the optical signatures of different many-particle charge complexes are only separated by up to tens of meV. For TMDs deposited on typical substrates such as SiO_2, the inhomogeneous broadening of spectral resonances of the order of several tens of meV makes it challenging—if not impossible—to optically resolve these signatures. Remarkably, encapsulation of the TMD monolayer by hBN leads to a narrowing of the inhomogeneous linewidth, unveiling a plethora of signatures in absorption and PL spectra arising from complex recombination processes of many-body compounds. In this section, we report on recent experiments probing trion and biexciton features in TMDs.

Trions, formed individually from an exciton and an additional electron or hole, have been observed in absorption and PL measurements.[59–62] Biexcitons[64–65]—consisting of two bound electron–hole pairs—and charged biexcitons[16,66–68]—biexciton plus an electron/hole—exhibit also features that could be observed in optical spectroscopy. In order to obtain a significant trion signal, the TMD must be doped. This can be achieved via intrinsic doping[69,70] or by the application of an external electric field.[66] Owing to the Coulomb interaction between the exciton and the electron/hole, the trion has a binding energy of ~20 – 30 meV and its spectral resonance is thus red-shifted from the corresponding exciton energy.[58,59] Moreover, absorption measurements show that the energy splitting between trion and exciton resonances increases with doping, providing a signature of the polaronic character of the exciton in the sea of doping charges.[62,71,72] For this reason, trion and exciton resonances are commonly denoted as attractive and repulsive polaron branches in absorption measurements. Recent studies[47,73] reported also the existence of dark trions at low temperatures in WSe_2. Similar to the excitonic case, they become visible via interaction with phonons. In these studies, the doping was controlled by an applied electric field resulting in three distinct regions of the PL dominated by dark excitons (low/no doping), dark positively charged trions (p-type doping), and dark negatively charged trions (n-type doping).

Figure 2(c) shows the PL spectrum around the bright exciton energy as a function of applied gate voltage for a hBN-encapsulated WSe_2 monolayer.[66] Due to the sharp lines, one can find a multitude of signatures including the neutral exciton (labeled X_0), positive trion (X^+), negative intervalley (X_1^-) and intravalley (X_2^-) trions, biexciton (XX), and negatively charged biexciton (XX^-). There is also clear emission from bound defect excitons (*D*). These states have been shown to enhance the PL intensity of the free exciton,[74] and they are important for the realization of single-photon emitters.[75–78] Through hBN-encapsulation, recent studies could even resolve the excited trionic 2s states.[79–81]

C. Exciton optics in TMD heterostructures

The two-dimensional nature of TMD monolayers encourages the vertical stacking of multiple TMD layers. The resulting structure, held together through the van der Waals interaction, inherits properties of the constituent monolayers. TMD homo-bilayers have typically an indirect bandgap due to a large hybridization of the states at the Λ and Γ valleys.[82] Unlike in monolayers, whose PL is dominated by the energetically lowest direct optical transition at room temperature, homo-bilayers[83] possess a rich structure of momentum indirect and direct excitons,[40] whose optical properties can be tuned via strain[84,85] or by an electric field.[85] Hetero-bilayers, formed from stacking two different TMD monolayers, can play host to interlayer excitons,[10] where the constituent electron and hole reside in different layers. The spatial separation of the electron and the hole strongly quenches the radiative recombination of these excitons, and, as such, they possess long lifetimes,[86,87] which is important for transport phenomena[88] and energy transfer processes in, e.g., solar cells.[89]

Interlayer excitons carry a permanent out-of-plane dipole moment, allowing their energy to be tuned via an electric field.[90–92] In PL and absorption measurements, this leads to a shift in the exciton resonance energy. Interestingly, interlayer excitons are also predicted to exist in homo-bilayers.[93] Moreover, these interlayer excitons strongly hybridize with the intralayer states, inheriting some of their oscillator strength, and are thus visible even at room temperature.[93,94] It was recently shown that by varying the gate voltage across the structure, the interlayer exciton resonance can be significantly tuned[94] [cf. Fig. 2(d)]. Concretely, the degeneracy of the two interlayer excitons is lifted, and their resonances move closer to the A1s and A2s intralayer excitons, respectively [cf. Fig. 2(e)].

In recent years, twisted TMD heterostructures have ignited substantial interest and given rise to the rapidly evolving field of semiconducting moiré superlattices.[3] Here, by tuning the twist angle between two or more stacked TMD layers, a new long-range periodicity can be created leading to novel electronic and excitonic properties.[95–98] The long-range moiré pattern manifests as a periodic network of potential wells,[99–102] trapping excitons when sufficiently deep. This trapping leads to the formation of distinct moiré exciton sub-bands, tens of meV below the free exciton energy level. Optically, this can be observed in the twist-angle dependent fine structure of both inter-[98] and intralayer[101,103] excitons. In addition, the structure of moiré excitons can be analyzed in detail in ARPES measurements. Concretely, the spatial extension of the exciton can be extracted from the momentum distribution of the ARPES

signal. In particular, interlayer excitons in WSe_2/MoS_2 structures with a twist angle of 2° were recently found to be localized within the 6 nm moiré unit cell.[104] Moreover, in the same structure but with a 10° twist angle, analogous experiments report the delocalized nature of interlayer excitons and their unique momentum fingerprint, which directly reflects the mini Brillouin zone of the moiré superlattice.[56]

Recent advances have shown that TMD-based moiré heterostructures undergo significant lattice reconstruction at low angles, leading to an even more complex network of trapped exciton domains[105,106] and giving rise to ferroelectric[107] and strain-induced effects.[108] Analogous to monolayer systems, homo- and heterobilayers exhibit higher-order charge complexes, such as moiré trions,[109–112] which appear in optical spectra as an additional fine structure of the trion peak. For more details about this exciting field of exciton research, we refer to a very recent review on moiré exciton effects.[3]

D. Exciton–polaritons

The interaction of excitons with light can be qualitatively modified by structuring the surrounding dielectric environment.[113] TMD monolayers and heterostructures are particularly relevant in the domain of nanophotonics as they are chemically stable at ambient conditions, do not suffer from lattice mismatch, and their exciton energy lies in the technologically relevant spectral region of visible and near-infrared, allowing for incorporation with a wealth of nanophotonic devices.[114] TMD nanophotonics can be divided into the weak and the strong coupling regime depending on the strength of the exciton–light interaction in comparison to the optical and material-based decay channels. In the former, losses dominate, and the (dressed) exciton remains a well-defined eigenmode of the system with a modified lifetime (Purcell effect). In other words, spectra can remain qualitatively unchanged, but exciton emission and absorption are enhanced/diminished via control of the local photonic density of states. For example, the low quantum yield of TMDs can be compensated by coupling to a suitably designed nanostructure to boost Raman and PL signals.[115,116] This not only can aid optical characterization of 2D materials,[117] but also has applications for ultra-compact optoelectronic devices based on excitons.[118,119] In a further example, it has been demonstrated that the weak absorption of monolayers ($\lesssim 10\%$)[120] can be greatly increased to near 100% using the Salisbury screen setup,[121,122] which could have utility for ultra-thin photovoltaics. In this section, we concentrate on TMDs in the strong-coupling regime,[114,118,123–125] focusing particularly on utilizing nanophotonics for sophisticated control of TMD exciton–polaritons, and the recent development of polariton twistronics.

The light–matter coupling strength of TMD heterostructures integrated into high-quality and small-volume optical microcavities can exceed both material dissipation and radiative decay from the cavity (both typically of the order of few to tens of meV), leading to coherent energy transfer between the exciton and cavity mode.[113] In this case, the system is in the strong-coupling regime and is characterized by the formation of hybrid quasi-particles, known as exciton–polaritons. These new eigenmodes of the combined light–exciton system inherit properties from their constituent parts, potentially combining the spatial coherence, small effective mass, and long propagation lengths of photons with the tunability and nonlinearity of material-based excitations.[126] In the frequency domain, the strong-coupling regime manifests as a splitting of the polariton energies, known as Rabi splitting [cf. Fig. 3(a)], which is determined by the strength of the light–exciton coupling and can be directly observed in angle-resolved linear optical spectroscopy.[113] The large oscillator strength of monolayer TMD excitons leads to an impressive Rabi splitting (up to ~50 meV in a typical dielectric microcavity[127]) in comparison to traditional polariton platforms such as GaAs quantum well microcavities (~4 meV for a single quantum well in a microcavity[128]). Furthermore, the large binding energy allows for robust room-temperature polaritonics. The study of exciton–polaritons in TMDs has led to a wealth of interesting phenomena, such as condensation of exciton–polaritons at cryogenic temperatures,[129] polariton lasing,[130] trapped[131] and Bloch polaritons,[132] motional narrowing,[133] and non-linear polariton parametric emission.[134]

The first demonstrations of the strong coupling regime in TMD monolayers used conventional dielectric Fabry–Perot cavities built from high-reflectivity distributed Bragg reflectors (DBRs),[127,135] hybrid DBRs plus silver mirrors,[136] and all-metal Fabry–Perot cavities built from silver mirrors.[137] Development of state-of-the-art fabrication methods allows for routine and precise construction on the nanoscale, meaning that the near- and far-field properties of light can be manipulated to form sophisticated cavities with controllable properties such as quality factor, field enhancement, polarization, and topology. For instance, Zhang *et al.* reported on a monolayer TMD placed on a 100 nm thick 1D photonic crystal slab.[138] Recording both angle-resolved reflectance and PL, convincing evidence of strong coupling physics has been found up to room temperature between WS_2 excitons and a guided mode supported by the structured slab [cf. Fig. 3(a)]. In another notable work,[139] exciton–polaritons were studied in a WSe_2 monolayer on a 2D SiN metasurface with a square lattice of holes. A strong directional polariton emission was measured in the far field due to the sub-wavelength structuring. Furthermore, a computational study demonstrated a highly tunable Rabi splitting, directional emission, and polariton dispersion via meta-atom engineering, such as changing lattice periodicity and slab thickness. For instance, excitons can couple to a photonic crystal mode with a "W-shaped" dispersion [cf. Fig. 3(b)]. In this case, the polaritons will inherit a negative effective mass and group velocity from the optical mode at normal incidence. This can lead to exotic polariton transport.[140] In another work, the strong coupling between excitons and a bound state in the continuum supported by a 1D photonic crystal slab was demonstrated.[141]

There is growing interest in exploring topological properties of polaritons.[142,144,145] One strategy toward this goal is coupling excitons to topologically non-trivial photonic systems,[145] which could lead to tunable optical devices that are robust against disorder and defects. Helical topological polaritons have been demonstrated using a WS_2 monolayer placed on a hexagonal photonic crystal[142] [cf. Fig. 3(c)]. While maintaining six-fold rotational symmetry, the unit cell can be expanded or shrunk to change the intercell and intracell nearest-neighbor couplings. This allows two bulk lattice regions to be engineered with different topological phases, with the boundary between the two supporting a topological interface mode.[145] This interface was found to support a topological

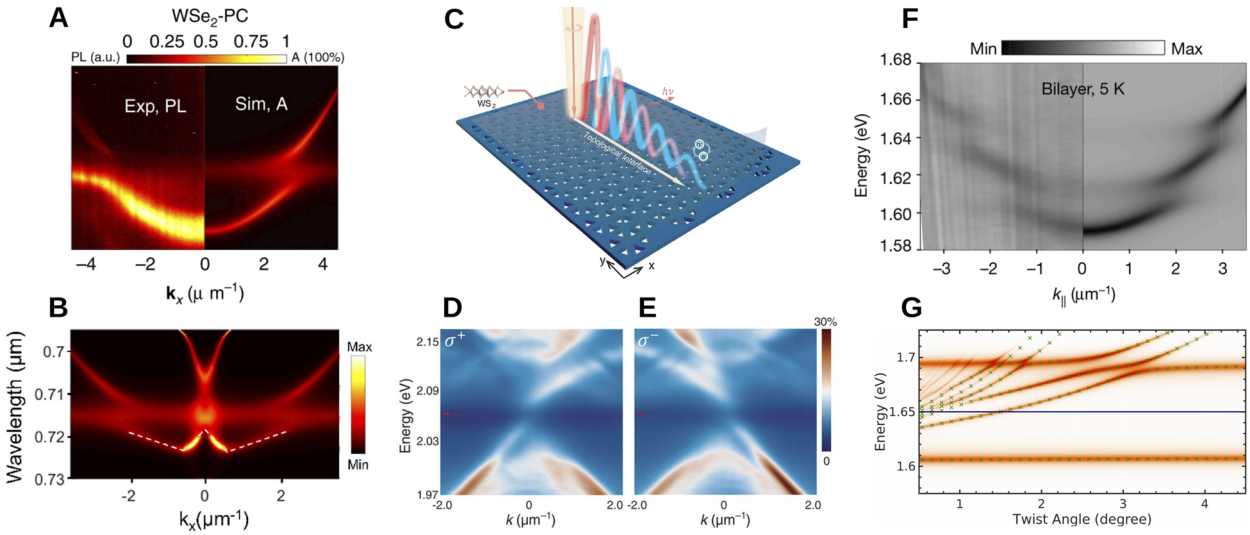

FIG. 3. Exciton–polaritons in TMD monolayers and heterostructures. (a) Experimental and simulated PL spectrum for a coupled monolayer TMD and photonic crystal slab in the strong coupling regime. (b) Simulated "W-shaped" dispersion of exciton–polaritons supported by a monolayer TMD on a metasurface, which is tunable via lattice periodicity and slab thickness. (c) Illustration of helical topological interface TMD exciton–polaritons. (d) and (e) Angle-resolved reflectance spectra of the interface polaritons excited by right/left-hand circularly polarized light. (f) First experimental evidence of strong coupling between two hybrid interlayer moiré excitons and a microcavity optical mode for a $MoSe_2/WS_2$ heterostructure, measured in angle-resolved reflection spectra. (g) Twist-angle dependence of polariton dispersion and absorption for a $MoSe_2/WSe_2$ heterostructure in a microcavity. Panels (a) adapted with permission from Zhang *et al*., Nat. Commun. **9**, 713 (2018). Copyright (2018) Springer Nature Ltd. Author(s) licensed under a Creative Commons Attribution 4.0 License; (b) adapted with permission from Chen *et al*., Nano Lett. **20**, 5292–5300 (2020). Copyright 2020 ACS; (c)–(e) adapted with permission from Liu *et al*., Science **370**, 600–604 (2020). Copyright 2020 AAAS; (f) adapted with permission from Zhang *et al*., Nature **591**, 61–65 (2021). Copyright 2021 Springer Nature Ltd.; (g) adapted with permission from Fitzgerald *et al*., Nano Lett. **22**, 4468–4474 (2022). Copyright 2022 ACS Author(s) licensed under a Creative Commons Attribution 4.0 License.

interface polariton due to the strong coupling between the photonic interface mode and the WS_2 exciton, or in an equally valid picture, as a consequence of the different topological phases of the bulk polariton bands in the two lattice regions. Crucially, the interface polaritons possess helical nature, i.e., the group velocity depends on the pseudospin of the polariton, which can be directly accessed via the circular polarization of incident light [cf. Figs. 3(d) and 3(e)]. Reference [142] demonstrates this unidirectional polariton transport in momentum space with reflection and PL measurements of the interface at temperatures 160–200 K.

Several unique aspects of TMD exciton–polaritons have been uncovered in recent years. Because of the large exciton binding energy, the temperature dependence of the exciton energy (via the bandgap[146]) can be used as a material-based detuning over a wide range of temperatures. In an early demonstration for monolayer WS_2, the light–exciton composition of polaritons was modified over the range 110–230 K, and could be inferred from angle-resolved PL.[147] As temperature was increased, the exciton energy was observed to red-shift, causing the lower polariton to shift from a photon-like state to an exciton-like state at small momenta. Strong coupling physics can also be modified through electric field induced gating of the TMD.[148] Here, by introducing electrostatically induced free carriers, the oscillator strength of the exciton decreases due to the screened Coulomb interaction between the constituent electrons and holes—this in turn leads to a reduced Rabi splitting. Furthermore, TMD exciton–polaritons were shown to inherit the valley physics of the constituent exciton.[149–151]

Research on valley polaritonics has emerged as a popular subfield, and numerous combined nanophotonic and valleytronic architectures have been explored.[152–154] In a notable example, it was shown that a condensate of exciton–polaritons in a hybrid monolayer $MoSe_2$–GaAs microcavity preserves valley polarization of the pump laser better than in the linear regime due to the speedup of the relaxation dynamics from the excitonic reservoir.[155] The large exciton binding energy and oscillator strength of TMD monolayer excitons has also opened up opportunities to explore polaritonics beyond the 1s exciton, offering insights into the many-body physics of TMDs[62] and the potential for highly nonlinear, exciton-based optical devices.[141,156,157] For example, the strong coupling between the 2s exciton in monolayer WSe_2 and the optical modes of a Fabry–Perot cavity have been demonstrated.[158] Strong coupling with trions has also been reported.[62,151,159–161] Because of their charged and composite fermionic nature, trion polaritons possess strong nonlinear behavior compared to neutral bosonic excitons.[162]

Recently, hybrid intra-interlayer moiré exciton–polaritons were explored in a H-stacked $MoSe_2/WS_2$ heterostructure with a twist angle of ~56.5° placed in a $\lambda/2$ microcavity.[163] Here, a twist-dependent interlayer hybridization means that the interlayer excitons inherit a large oscillator strength from the $MoSe_2$-based intralayer excitons at small twist angles.[164] It was found that the two bare moiré excitons coherently couple to the cavity mode to form three moiré polariton branches, which are measured with angle-resolved reflection and PL [cf. Fig. 3(f)]. In other words, the

moiré polaritons in this system are a three-way coherent coupling between a cavity photon and the bare intra- and interlayer moiré excitons. Relative to monolayer exciton–polaritons, these hybrid moiré polaritons show negligible energy shift, smaller line-broadening, and much stronger reduction in the Rabi splitting with increasing excitation densities. These observations are attributed to the zero dimensionality of the moiré exciton and a consequent exciton blockade effect.[165] Localization of the exciton at the potential minima in each moiré supercell can be expected to lead to enhanced exchange and dipole–dipole interactions (via the interlayer component). This extra energy cost of adding an exciton to a moiré cell leads to a suppression of many-body effects and the exciton–photon coupling saturating at one exciton per moiré cell. This study presents an exciting first step toward "polaritonic twistronics." Unfortunately, experiments are typically limited to a few fixed twist angles, while in theoretical studies, one can map out the moiré exciton–polariton energy and absorption over a wide range of twist angles, as recently demonstrated for the specific case of the purely intralayer exciton–polaritons of a twisted type II $MoSe_2/WSe_2$ heterostructure in a microcavity using a combined Wannier plus Hopfield method[166] [cf. Fig. 3(g)]. Furthermore, theoretical studies have looked at possible topological transport properties of interlayer exciton–polaritons in a cavity,[167] while a Bose–Hubbard model has been used to explore moiré-induced optical nonlinearities,[168] and a quantum-electrodynamical extension of the Bethe–Salpeter method has been used to explore an interesting photon-induced reordering and mixing of intra- and interlayer excitons in an untwisted MoS_2/WS_2 bilayer.[169]

III. EXCITON DYNAMICS

The dynamics of exciton formation, thermalization, and recombination, crucially, determines the performance of TMD-based optoelectronic devices. For instance, the thermalization of excitons into long-lived dark states in tungsten-based TMDs results in the suppression of the PL, making these materials undesirable for light-emitting applications, but suitable for light harvesting. Similarly, non-radiative recombination processes, such as exciton–exciton annihilation, can significantly limit the quantum yield. At moderate doping levels or large exciton densities, many-body complexes, such as trions or biexcitons, become relevant and dominate the thermalization and recombination dynamics. Moreover, in TMD heterostructures, charge transfer arises as a major thermalization mechanism, and the exciton recombination dynamics becomes significantly influenced by the stacking and the twist angle of the constituent layers. In this section, we summarize the recent progress in the understanding of these important processes.

A. Exciton formation and thermalization

Recent advances in two-photon photoemission spectroscopy (2PPS), also known as time-resolved ARPES (tr-ARPES), have enabled the direct observation of exciton formation and thermalization in energy, momentum, and time.[53,55–57,170] In this technique, an initial pump pulse photoexcites electrons from the valence band to the conduction band, resulting in the formation of excitons. After a certain time delay, the excitons' constituent electrons are photoemitted by a second pulse, and their energy and momentum are then measured by a hemispherical analyzer or a time-of-flight momentum microscope.[170] The detected electrons directly reflect the exciton population and, importantly, their momentum configuration. Thus, ARPES allows for the direct visualization even of momentum-dark excitons, which are not directly accessible in PL or optical absorption spectra.

The formation of momentum-dark excitons in WSe_2 monolayers has been resolved in a very recent tr-ARPES study.[53] First, electrons and holes at the K point are optically excited, leading to an almost immediate signal arising from photoemitted electrons with momentum K [cf. Figs. 4(a) and 4(b)]. After a delay of 0.4 ps, electrons with momentum Λ (also commonly denoted Q or Σ in literature) and energy similar to those at the K point are detected. The measured energy of Λ electrons is significantly lower than the energy predicted by *ab initio* calculations of the single-particle band structure. However, due to their large binding energy, momentum-dark KΛ excitons (formed by a hole at the K point and an electron at the Λ point) have been predicted to reside energetically below the bright KK states.[9,42,55,171,172] In other words, the observed Λ electrons are bound to holes at the K valley and thus form momentum-dark KΛ excitons. The delay between the appearance of K and Λ electrons is, therefore, a direct reflection of the intervalley exciton–phonon scattering, which is responsible for the thermalization of the exciton population in the multi-valley band structure of TMDs.[55,172] The measured delay of 0.4 ps thus quantifies the exciton–phonon scattering time at the considered temperature of 90 K. Another experiment has been performed for monolayer WS_2,[55] where similar energy of KK and KΛ excitons was resolved and an intervalley scattering time of 16 fs at room temperature was extracted. The definite proof that photoemitted electrons arise from bound exciton states relies on the direct visualization of the exciton wave function and the theoretical prediction of an inverted dispersion relation for the photoemitted electron.[171] Both features have been successfully observed in monolayer[173] and bulk[57] WSe_2. These recent studies investigating exciton formation with tr-ARPES confirm the importance of momentum-dark KΛ excitons in tungsten-based TMDs and provide a direct quantification of the intervalley exciton–phonon scattering time in these materials.

The exciton thermalization dynamics can also be probed indirectly via the optical absorption and emission characteristics of the material.[37,38,174–177] Initial studies focused on resolving the valley and spin depolarization after a circularly polarized optical excitation.[178–181] Other studies have utilized indirect signatures of dark excitons in optical spectroscopy to track their formation. For example, optical-pump THz-probe experiments can be performed to resolve the exciton dynamics by exploiting the temporal evolution of the 1s-2p exciton transition resonance.[174,182] In particular, the blue-shift of the 1s-2p THz resonance peak reflects the sub-picosecond relaxation of bright KK excitons into the lower-lying momentum-dark KΛ state, which displays larger 1s-2p resonance energy.[175] The formation dynamics of dark excitons have also been indirectly resolved by tracking the emergence of phonon-assisted PL peaks at cryogenic temperatures.[176]

The exciton formation can also be resolved by exploiting the population-induced changes in the optical absorption.[37,38,177] In particular, above-band optical excitation provides a unique fingerprint to track the relaxation cascade into the exciton ground state.[37,38]

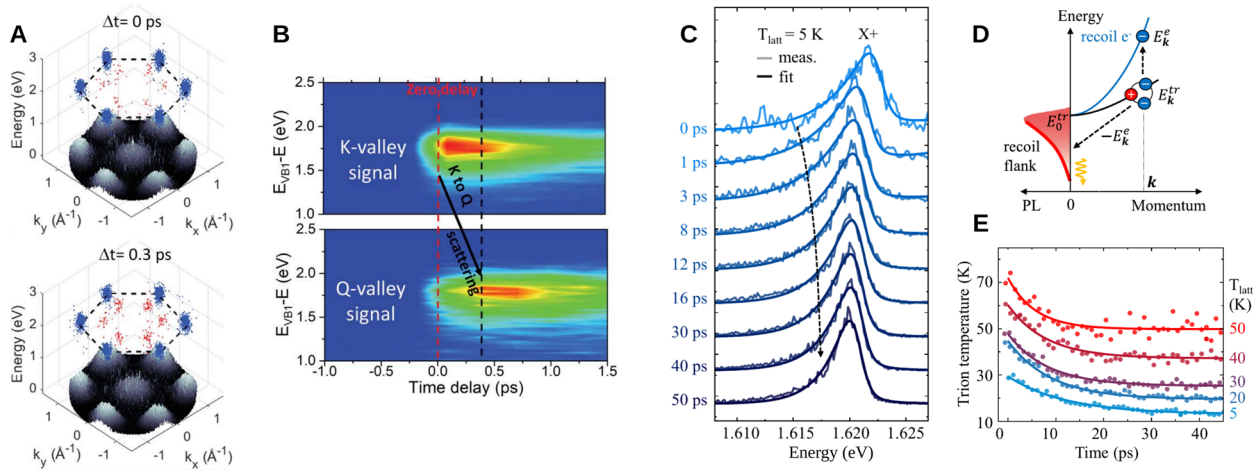

FIG. 4. Exciton and trion dynamics in monolayer TMDs. (a) ARPES maps of the electron occupation in the conduction and valence bands during (0 ps) and shortly after (0.3 ps) optical excitation. (b) Time-resolved energy scan of the ARPES signal at the K and Λ (Q) valleys illustrating the thermalization of excitons into the dark KΛ states. (c) Time snapshots of the trion PL, displaying an asymmetric broadening that can be traced back to the trion temperature. (d) Schematic illustration of trion recombination and the electron recoil effect. (e) Time evolution of the extracted trion temperature for different lattice temperatures, demonstrating trion cooling. Panels (a) and (b) adapted with permission from Madéo *et al.*, Science **370**, 1199–1204 (2020). Copyright 2020 AAAS; (c)–(e) adapted with permission from Zipfel *et al.*, Phys. Rev. B **105**, 075311 (2022). Copyright 2022 APS.

Signatures of efficient phonon cascades that would enable this process have been recently observed.[183] The opposite process of exciton dissociation can occur via an external electric field[184] or by scattering with phonons[185] and crucially limits the performance of TMD-based optoelectronic devices.

B. Exciton recombination

Having binding energies in the range of hundreds of meV, excitons govern the dynamics of electron–hole recombination in monolayer semiconductors and vdW heterostructures. Depending on the dielectric environment and excitation power, excitons mainly recombine radiatively by emitting photons or non-radiatively by other processes, e.g., via defect-assisted recombination or exciton–exciton annihilation.[186,187] Radiative recombination in monolayers has been extensively studied in the past,[36,182,188,189] with the hallmark being the characteristic temperature-dependence of the recombination time in tungsten- and molybdenum-based TMDs, owing to the dominance of dark excitons in the first case and bright excitons in the second.[41,172] More recently, the radiative lifetime has been found to be tunable with the thickness of the hBN-encapsulation layers due to the Purcell effect.[116]

Electron–hole pairs can also recombine via non-radiative recombination processes, such as exciton–exciton annihilation (EEA), at elevated exciton densities,[187,190–197] and defect-assisted recombination.[187,198–200] EEA crucially limits the efficiency of optoelectronic devices, as it leads to a saturation of the quantum yield with increasing carrier density. Nevertheless, it also presents an opportunity for photon upconversion.[193,201] In this Auger-like recombination process, one exciton recombines, by transferring its energy and momentum to another exciton. In order for this mechanism to occur, energy- and momentum-conservation must be fulfilled. This implies that the efficiency of EEA is highly sensitive to the excitonic band structure, which contains the suitable final states. In fact, the EEA rate has been found to vary significantly with the dielectric environment[187,194,195] and strain.[197] In particular, EEA was demonstrated to be highly inefficient in hBN-encapsulated WS_2, displaying an EEA rate of 0.004 cm^2 s^{-1} compared to 0.4 cm^2 s^{-1} for samples deposited on SiO_2 substrates.[187] The large EEA rate in TMD/SiO_2 structures has been suggested to partially originate from the relaxed energy- and momentum-conservation due to the strong dielectric disorder in these structures.[187] More recently, a microscopic model showed that the band structure in TMD/SiO_2 structures is more favorable for EEA due to the optimal energy of the higher-lying exciton state.[193,196,201] In addition, the modification of the band structure via tensile strain has been recently shown to efficiently suppress EEA in monolayer WS_2 on a SiO_2 substrate.[197]

C. Trion and biexciton dynamics

In the presence of doping, trions govern the dynamics in TMDs. A lot of research is currently focusing on characterizing and understanding the dynamics of trion formation and thermalization. Initial studies resolved the formation of trions in pump–probe spectroscopy and determined a formation time of about 2 ps at cryogenic temperatures.[202,203] At the same time, the spin–valley depolarization dynamics was extensively studied,[58,60,204,205] with key studies reporting a very long-lived valley coherence for trions in MoS_2[58] and WSe_2.[205] Recently, the role of excited trion states has been investigated. In particular, it was found that 2s excitons bound to a doping charge can relax into the ground 1s exciton state on a timescale of 60 fs, transferring the excess energy to the doping charge in a process denoted as autoionization.[80]

Trions exhibit a characteristic recombination mechanism in which one electron–hole pair recombines and the trion's center-of-mass momentum is transferred to the remaining charge carrier, which then becomes free [cf. Fig. 4(d)]. This phenomenon is known as the electron recoil effect[206] and leads to an asymmetric broadening of the trion PL, as opposed to the symmetric broadening usually displayed by bright-exciton PL. Importantly, the broadening of the low-energy tail of the trion PL is determined by the temperature of the trion gas.[207,208] While the electron recoil effect has been known for a long time,[59,206,208] it has been exploited to extract the trion temperature and resolve the cooling of the trion population after an optical excitation only recently.[207] In Fig. 4(c), time snapshots of the trion PL in $MoSe_2$ are shown.[207] Immediately after the optical excitation, the trion PL displays a broad low-energy tail that shrinks on a 10 ps timescale. The shrinking is a direct manifestation of the trion temperature cooling down and reaching an equilibrium with the thermal bath of lattice phonons [cf. Fig. 4(e)]. These measurements can be systematically used to study how the trion cooling dynamics is affected by external knobs, such as lattice temperature and doping. In fact, the cooling time was found to be approximately constant (~10 ps) up to 40 K. At higher temperatures, the thermal activation of optical and zone-edge acoustic phonons enhances the trion–phonon scattering, resulting in faster cooling rates. While trion–phonon scattering is the dominant cooling mechanism up to doping levels corresponding to a hole density of 3×10^{11} cm^{-2}, scattering between trions and free carriers becomes relevant at larger doping levels and further reduces the cooling time. The microscopic mechanisms governing trion–phonon interactions have been recently studied in a theoretical work.[209]

Understanding the main trion recombination pathways is crucial for efficient doping tunability of optical devices. The trion recombination time in $MoSe_2$ monolayers was found to change significantly with temperature, varying from 15 ps at 7 K to sub-picosecond timescales above 100 K.[188] This strong temperature dependence was suggested to be caused by the thermal activation of phonon-assisted trion dissociation into an exciton and a free electron. Recent studies have estimated the non-radiative recombination time of trions in molybdenum-based TMDs to be typically around 50–100 ps, i.e., competing or even dominating over the radiative lifetimes of 100 ps[116] and 100 ns[200] that have been reported in $MoSe_2$ and MoS_2, respectively. The significant discrepancy in the trion recombination times among different studies highlights the need for a better understanding of this process. In particular, future studies should be carried out at carefully controlled experimental conditions and be accompanied by theoretical models accounting for both radiative and non-radiative recombination mechanisms.

At high exciton densities, more complex many-particle compounds, such as biexcitons, can become relevant. The spin–valley configuration of optically accessible biexciton states, as well as the characteristic quadratic dependence of the PL with pump power, has been reported.[16,64,67,210] In particular, bright biexcitons were found to be composed of one KK and one K′K′ exciton with the opposite spin configuration in WSe_2 monolayers.[64] More recently, biexciton recombination and exciton–exciton scattering were predicted to be largely tunable by external magnetic fields.[65] In the presence of an in-plane or tilted magnetic field, the spin selection rules for biexciton recombination and exciton–exciton interaction are relaxed, allowing for more recombination and scattering channels.

D. Exciton dynamics in TMD heterostructures

TMD heterostructures offer a platform to spatially separate charge carriers. The resulting charge-separated state, i.e., the interlayer exciton or charge-transfer exciton, has characteristic properties that can be utilized to modify the optical response and transport properties of the material. In this section, we summarize the recent developments in the understanding of the charge transfer process in TMD heterostructures. Moreover, we discuss the recombination dynamics in these systems and the impact of the twist angle between two TMD layers.

Following the characterization of exciton formation and thermalization in monolayer TMDs, efforts have been directed toward investigating the dynamics of charge transfer and the formation of spatially separated interlayer excitons in vdW heterostructures.[56,211,212] The formation dynamics of interlayer excitons has been tracked in tungsten-based heterostructures using optical-pump THz-probe spectroscopy at room temperature.[213] The density of intra- and interlayer excitons can be accessed by measuring the THz conductivity at the 1s-2p transition energy of each exciton species [cf. Fig. 5(a)]. The time-resolved THz conductivity is shown in Fig. 5(b). The initial optical excitation generates intralayer excitons in the WSe_2 layer, which becomes manifest as a peak in the THz spectrum at the 1s-2p transition energy of 150 meV.[213] At the same time, a low-energy peak at ~70 meV originating from interlayer excitons emerges, indicating that the charge-transfer occurs on a sub-picosecond time scale. After the optical excitation, the intralayer exciton peak vanishes, while the interlayer exciton resonances become more prominent as the whole exciton population relaxes into this energetically favorable state. These features reflect the transfer of electrons from the WSe_2 layer to the WS_2 layer, resulting in the formation of interlayer excitons with an excess energy that is later dissipated into the phonon bath.[214] Intriguingly, the time scale of charge-transfer strongly depends on the stacking angle of the vdW heterostructure. This effect has been shown to arise from the momentum offset between intra- and interlayer exciton dispersions [cf. Fig. 5(c)].

The charge transfer process in WSe_2/MoS_2 moiré lattices has been recently resolved directly in tr-ARPES experiments,[56] revealing an ultrafast sub-50 fs tunneling time scale. It was found that the charge transfer is a two-step process, where optically excited WSe_2 intralayer excitons first scatter with phonons into the strongly hybridized momentum-dark KΛ excitons (where electrons are delocalized over both layers). In a second step, these hybridized excitons scatter into the energetically lowest interlayer exciton states, where the electron is located in the $MoSe_2$ layer. The charge transfer process is sensitive to temperature, as it is mediated by phonons, and strongly depends on the stacking, as this determines the energy landscape of excitons.[56,102,215]

Apart from vdW heterostructures consisting exclusively of individual TMD monolayers, TMD-graphene structures have also been extensively studied due to their technological relevance.[216–222] In particular, TMD and graphene can be stacked together to form optoelectronic devices such as photodetectors or solar cells, where the TMD acts as an optical absorber and graphene acts as a

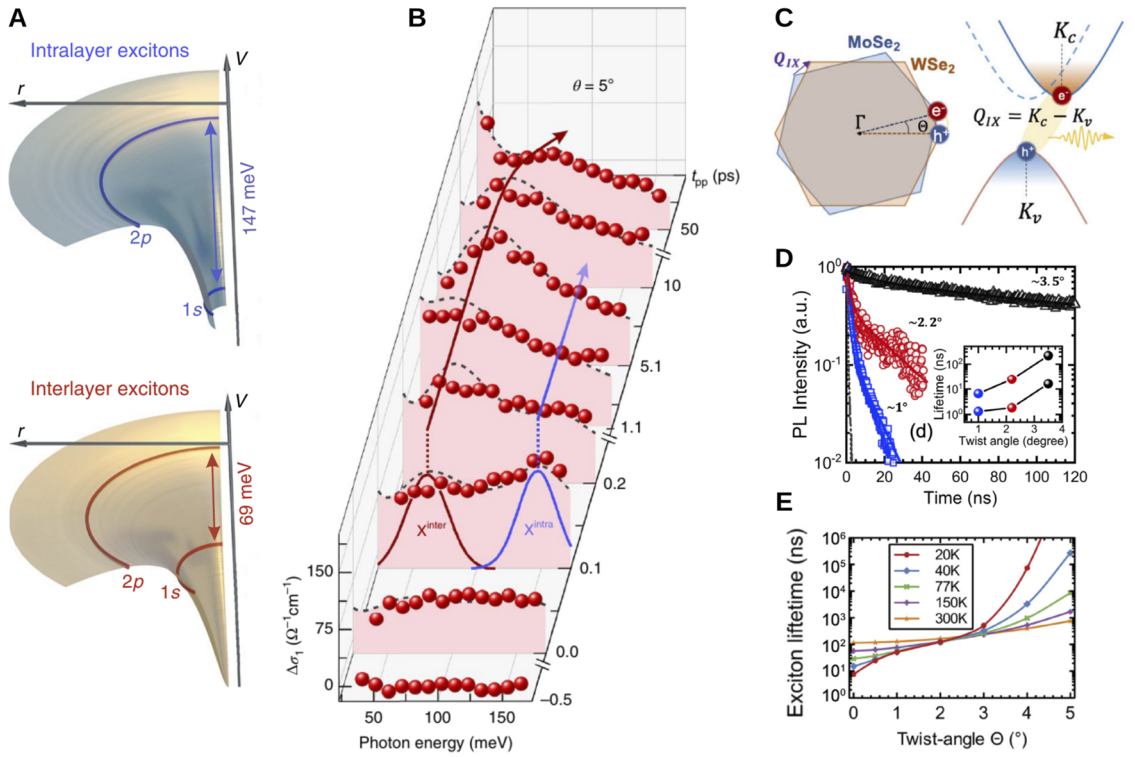

FIG. 5. Exciton dynamics in TMD heterostructures. (a) Intra- and interlayer Coulomb potential, together with the energetic position of the 1s and 2p exciton states in a tungsten-based vdW heterostructure. (b) Time- and energy-resolved pump-induced change of the optical conductivity in an almost aligned (5° twist angle) heterostructure, illustrating the transition from an intra- to an interlayer exciton. (c) Schematic representation of the $MoSe_2$ and WSe_2 Brillouin zones twisted with respect to each other (left panel). The finite twist angle makes the interband transition in this heterostructure indirect (right panel). (d) PL intensity in $MoSe_2/WSe_2$ heterostructures as a function of time for different twist angles. The time evolution of the PL is fitted with a bi-exponential function and the extracted lifetimes are displayed in the inset. (e) Predicted exciton lifetime as a function of twist angle for different temperatures. Panels (a) and (b) adapted with permission from Merkl *et al.*, Nat. Mater. **18**, 691–696 (2019). Copyright 2019 Springer Nature Ltd.; (c)–(e) adapted with permission from Choi *et al.*, Phys. Rev. Lett. **126**, 047401 (2021). Copyright 2021 APS.

transparent contact.[223,224] In a recent study, the charge transfer in WS_2/graphene structures, after an optical excitation of excitons in the WS_2 layer, was found to occur on a sub-picosecond time scale.[220] Such ultra-fast charge transfer from TMDs to graphene has recently been shown to lead to a complete neutralization of the TMD and thus to a filtering of the PL spectra displayed by these structures.[219] Instead of the complex PL spectra of TMD monolayers, which involve trions and charged biexcitons, TMD-graphene heterostructures exhibit single narrow PL peaks arising from radiative recombination of neutral excitons. Furthermore, the asymmetry between the electron and hole transfer leads to a charge-separated state that can last between 1 ps[220,221] and 1 ns.[222] The charge-transfer process in WS_2/graphene was suggested to occur directly at the band intersection around the K point of the two layers. Crucially, the higher energy barrier and suppressed tunneling strength for electrons hinder their tunneling from WS_2 into the graphene layer, whereas holes can efficiently tunnel and relax into the graphene Dirac cone.[221] In addition, defects in the TMD layer have been suggested to modify the charge separation lifetime by trapping the electrons into localized states.[221,222]

While radiative recombination in TMD heterostructures has been studied for a few years,[10,86,87,90,225,226] only recently its twist-angle dependence has been characterized and understood on a microscopic footing.[227] Importantly, the twist angle determines the momentum offset between the conduction band minimum and the valence band maximum of the two layers [cf. Fig. 5(c)]. As the transition becomes more indirect, radiative recombination becomes less efficient, resulting in a longer exciton lifetime for larger twist angles [cf. Fig. 5(d)]. Moreover, the moiré potential significantly impacts the radiative lifetimes, by relaxing the momentum conservation of the recombination process and modifying the energy landscape of moiré excitons. The radiative lifetime was found to increase by one order of magnitude when increasing the twist angle from 1° to 3.5° in $MoSe_2/WSe_2$ heterostructures.[227] Due to the different energy landscape of moiré excitons at small and large twist angles, the radiative lifetime displays an opposite temperature dependence in these two regimes. At small twist angles, the light cone becomes depleted for increasing temperatures, resulting in a longer lifetime, while at large twist angle, the opposite occurs [cf. Fig. 5(e)].

Non-radiative recombination via Auger scattering has been suggested to be suppressed in TMD homo-bilayers due to the hybrid nature of the exciton, which coexists in both layers.[96,192,213,228] In fact, the EEA rate was found to decrease from 0.4 $cm^2\ s^{-1}$ in WSe_2 monolayers to 0.006 $cm^2\ s^{-1}$ in bilayers.[192] Intriguingly, Auger scattering has been suggested to be enhanced with an out-of-plane electric field that polarizes excitons and effectively increases the exciton–exciton interaction.[229] A more recent work has attributed the bimolecular recombination observed at high densities in WSe_2 bilayers to the recombination of unbound electron–hole pairs.[228] This has been exploited to resolve the Mott transition, which was measured to occur around $7.4 \times 10^{12}\ cm^{-2}$ in such structures. Above this density, electron–hole pairs are unbound and the dynamics is governed by electron–hole plasma.[230]

IV. EXCITON TRANSPORT

Exciton dynamics in atomically thin semiconductors has been intensely studied for more than a decade, following the first successful exfoliation of TMD monolayers. However, the spatiotemporal dynamics of excitons has been put in the focus of 2D material research only recently.[231–235] The understanding of exciton propagation is crucial for potential applications of TMD monolayers and heterostructures that could rely on the controlled transport of excitons in the material. Importantly, while excitons are charge-neutral particles, their spatial propagation can be directed by potential gradients generated by, e.g., inhomogeneous strain.[236] Being able to track excitons in space and time is of key importance for the successful development of TMD-based devices as it enables the opportunity to directly manipulate exciton currents. In this section, we summarize the recent developments on exciton transport, with focus on exciton diffusion and funneling in TMD monolayers, as well as in vertical and lateral heterostructures.

A. Exciton diffusion

Excitons are commonly tracked in both space and time by means of spatiotemporal photoluminescence measurements.[187,231,232,237] As schematically shown in Fig. 6(a), excitons form after optical excitation, and then propagate and scatter. After some time, a fraction of excitons recombines radiatively, emitting light at a finite distance from the initial excitation spot. In Fig. 6(b), a streak camera image of the PL for a low excitation density is shown, revealing a signal that decays with time and broadens in space. Quantitatively, in the low-excitation regime, the PL intensity $I_{PL}(x,t)$, being directly proportional to the exciton density $n(x,t)$, can be fitted to a Gaussian $\sim \exp(-x^2/\sigma_t^2)$, where $\sigma_t^2 = 4Dt + \sigma_0^2$ is the spatial variance and D is the diffusion coefficient. The spatial variance changes linearly with respect to time and the Gaussian shape of the exciton density $n(x,t)$ is retained for all times t. This spatiotemporal behavior can be explained by the Fick's law for diffusion[238] $\partial_t n = D\nabla^2 n$, which can be recovered from the full state-dependent Boltzmann equation of the spatiotemporal exciton dynamics in the limit of fast scattering and quasi-thermalized local distributions.[239,240] In this thermalized regime and in the limit of state-independent scattering times τ, the diffusion coefficient becomes $D = k_B T\tau/M$, with T and M being temperature and total exciton mass, respectively.[239,240] More recently, low-temperature deviations from this simple temperature dependence of D have been observed and attributed to quantum interference effects.[241,242] Therefore, the transport behavior observed in Fig. 6(b) at low excitation powers is commonly referred to as conventional or regular diffusion. This takes place after the excitons have reached a thermal equilibrium, while, before that, excitons exhibit ballistic propagation ($\sigma_t^2 \propto t^2$) and transient diffusion.[240,243]

When increasing the excitation density in the considered WS_2 monolayer, a halo-like pattern emerges in the spatial PL map, which indicates that excitons quickly move out of the excited high-density region,[232] cf. Fig. 6(b), center and right column. The now time-dependent effective diffusion coefficient $D_{\text{eff}}(t) = \frac{1}{4}\frac{d}{dt}\sigma_t^2$ was observed to increase from 0.3 cm^2/s at low excitation densities (below $n_x = 10^9\ cm^{-2}$) up to 20 cm^2/s at a moderate exciton density of $n_x = 10^{11}\ cm^{-2}$.[232] The microscopic mechanism governing the formation of exciton halos and the unconventional non-linear diffusion observed in TMD monolayers at elevated exciton densities[232,233,244,245] has been ascribed to the formation of strong spatial gradients in the exciton temperature.[232,246] Such temperature gradients are caused by the scattering of excitons with hot phonons that are created during the relaxation cascade of high-energy Auger-scattered excitons. These high-energy excitons are the result of efficient Auger scattering. While the gradient in the exciton temperature explains the observed diffusion and halo formation at room temperature, another phenomenon—the phonon wind effect—has been predicted to play a relevant role in the formation of halos at cryogenic temperatures.[246] In this effect, phonons created during the relaxation of Auger-scattered excitons propagate ballistically, dragging excitons out of the excitation spot. Similar non-linear diffusion[247] and halo formation[248] have been reported in monolayer MoS_2 and were suggested to arise from screening of the exciton–phonon interaction by trapped charges and from the formation of an electron–hole liquid, respectively.

Apart from excitation density, exciton diffusion can also be controlled via dielectric engineering,[14,187,249,250] strain,[197,251,252] or gating.[237,253] The energy landscape of excitons, consisting of bright and dark exciton states, is highly sensitive to both strain[254,255] and changes in the dielectric environment.[256] Comparing TMD layers deposited on a SiO_2 substrate with hBN-encapsulated samples, the latter display weak dielectric disorder leading to a faster diffusion.[14,187,250] Moreover, strain can alter the relative positions of different excitonic valleys,[257,258] resulting in a strain-controllable closing of scattering channels, giving rise to diffusion coefficients increased by a factor of 3 with about 0.6% biaxial strain.[252] Finally, gating can be used to disentangle neutral exciton diffusion from contributions to the diffusion due to unintentional doping and trions.[237,253]

In recent years, also the transport and propagation of quasiparticles beyond excitons has been studied extensively. Interestingly, the propagation of exciton–polaritons is strongly influenced by their excitonic or photonic nature. For example, exciton–polaritons in WSe_2 waveguides were observed to propagate at a velocity of $0.017c$, where c is the speed of light.[259] In other words, photons are significantly slowed down when they interact strongly with excitons. Moreover, thanks to the long propagation lengths

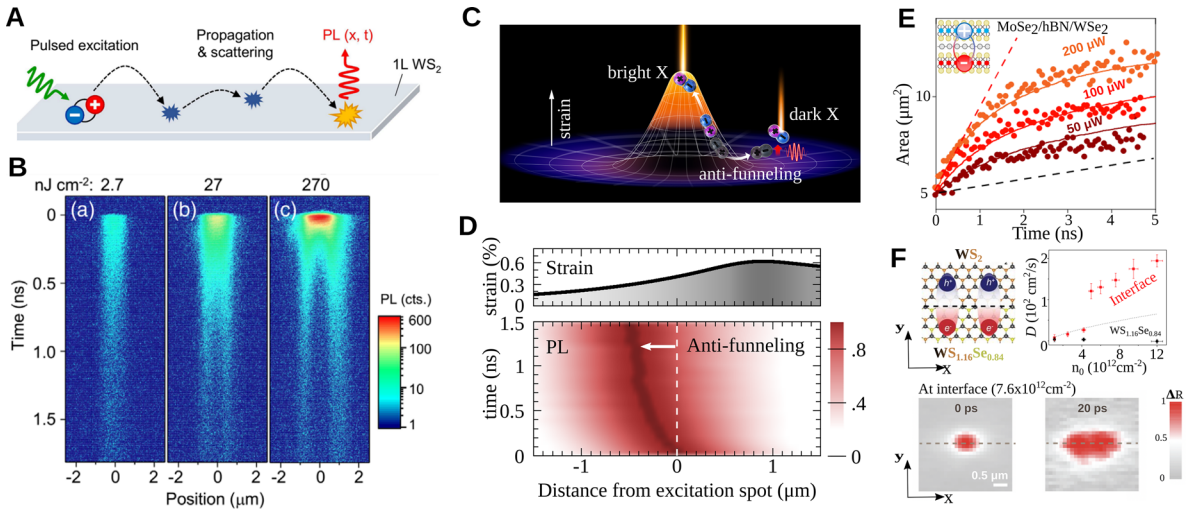

FIG. 6. Exciton transport in TMD monolayers and heterostructures. (a) Schematic illustration of exciton propagation and recombination in TMD monolayers. (b) Space- and time-resolved PL for a supported WS_2 monolayer, revealing the formation of a halo-like profile at large pump power densities. (c) Schematic illustration of exciton funneling of bright excitons and anti-funneling of dark excitons. (d) Strain profile (top) and spatiotemporal evolution of the exciton PL (bottom) in monolayer WS_2, showing the anti-funneling of excitons toward regions of low strain, attributed to the drift of dark KΛ excitons. (e) Time evolution of the exciton area (spatial variance) for different pump powers, demonstrating the anomalous diffusion of interlayer excitons in $MoSe_2$-hBN-WSe_2 heterostructures. (f) Schematic illustration of CT excitons in lateral heterostructures (top left). Differential reflection maps at 0 and 20 ps along the interface (bottom), demonstrating exciton diffusion in lateral heterostructures. Extracted diffusion coefficient as a function of electron–hole density (top right), revealing an abrupt increase of the spatial-spread speed after high-power excitation at the interface. Panels (a) and (b) adapted with permission from Kulig *et al.*, Phys. Rev. Lett. **120**, 207401 (2018). Copyright 2018 APS; (c) and (d) adapted with permission from Rosati *et al.*, Nat. Commun. **12**, 7221 (2021). Copyright 2021 AAAS Author(s), licensed under a Creative Commons Attribution 4.0 License; (e) adapted with permission from Sun *et al.*, Nat. Photonics **16**, 79–85 (2022). Copyright 2022 Springer Nature Ltd.; (f) adapted with permission from Yuan *et al.*, arXiv:2111.07887 (2021). Copyright 2021 AAAS Author(s), licensed under a Creative Commons Attribution 4.0 License.

of exciton–polaritons with a small effective mass, the optical valley Hall effect has been demonstrated in $MoSe_2$ embedded in a microcavity.[260] Trions also provide an intriguing platform for charge transport, as they acquire the large oscillator strength of the exciton and the charge of the extra electron or hole. In fact, the drift of trions under the influence of an electric field has recently been observed.[253] Here, a slow diffusion coefficient of 0.47 cm^2/s and a drift velocity of 7400 cm/s were reported in a WS_2 monolayer at cryogenic temperatures. Other studies have investigated trion diffusion and reported substantially different diffusion coefficients ranging from the 0.47 cm^2/s mentioned above up to 18 cm^2/s,[237,261] with signatures of even faster diffusion at cryogenic temperatures.[245] While a recent theoretical work has studied the impact of trion–phonon scattering on trion transport,[209] a microscopic understanding of trion diffusion in different regimes is still lacking.

B. Exciton funneling

Current nanoelectronics relies on controlling the charge transport within the device. While for charge carriers this can be achieved by applying electric fields, other mechanisms are required to spatially guide neutral excitons. Strain engineering provides a way of manipulating exciton propagation in TMDs, since the band structure of these materials is remarkably sensitive to strain.[257,258] In particular, strain is seen to induce significant energy shifts of exciton resonances.[254,255] Localized strain profiles as obtained, e.g., via ripples,[262] bubbles,[263–265] pillars,[266,267] or patterned substrates,[268,269] result in space-dependent exciton energies $E \equiv E(\mathbf{r})$ as reflected by spatially resolved spectra. Since the excitons move toward the spatial positions where their energy is minimal, their transport after thermalization can typically be described by a drift–diffusion equation

$$\partial_t n(\mathbf{r},t) = \nabla \cdot (D \nabla n) + \nabla \cdot (\mu n \nabla V(\mathbf{r},t)), \tag{1}$$

where $n(\mathbf{r},t)$ is the spatial- and time-dependent exciton density and μ is the exciton mobility, which can be approximated at low densities as $\mu \approx \frac{D}{k_B T}$. The first term in Eq. (1) corresponds to the Fick's law of diffusion.[238] The second term describes the drift induced by a potential V, which could have different microscopic origin, e.g., inhomogeneous strain, gating, or repulsive dipole–dipole interactions in heterostructures.[234,270,271] In the case of locally strained monolayers, the drift force is caused by strain-induced variations of exciton energy $\nabla E(\mathbf{r})$, cf. Fig. 6(c).

The spectral analysis of time-integrated photoluminescence in rippled few-layer MoS_2 revealed how localized strain profiles act as excitonic traps.[262] In particular, the relation between photoluminescence resonance and strain reveals that excitons funnel before recombining.[262] Excitons funnel toward regions with maximum strain, which results in an enhancement of the PL intensity in these regions.[266,272] Recently, the exciton drift has been experimentally tracked by means of space- and time-resolved photoluminescence measurements.[236,273,274] Exciting far away from a strain profile induced, e.g., by a pillar, the PL becomes broader in space without shifting its central position.[273] In other words, only

diffusion is observed (without drift/funneling) due to the absence of local strain profiles close to the excitation spot.[273] The situation differs significantly when the excitation is performed in strained regions, i.e., close to the pillar. In this case, the time-resolved PL profiles reveal exciton motion toward the center of the pillar, where the strain is maximized, by hundreds of nanometers in the first nanosecond.[273] Space- and time-resolved PL has been applied also to strain profiles dynamically altered by a tip.[274] In this way, it has been shown how the tip-induced strain can literally steer the motion toward the maximum-strain positions.[274]

More recently, exciton anti-funneling has been reported,[236] with excitons moving toward regions of low strain, see Fig. 6(d). This surprising behavior was observed in WS_2 deposited on a borosilicate substrate with an array of polymer micropillars, in contrast to analogous experiments performed on $MoSe_2$.[236] This can be understood in terms of the rich exciton landscape in TMD monolayers. While the energies of bright (KK) states decrease with increased strain, the opposite holds for momentum-dark KΛ intervalley excitons.[257,258] The strain-induced variation $\nabla E_v(\mathbf{r})$ of the energy $E_v(\mathbf{r})$ in the exciton valley v = KK, KΛ thus induces opposite drift forces for bright (KK) and dark (KΛ) exciton species. This complex interplay between bright and dark exciton propagation can be described by generalizing the drift–diffusion Eq. (1) to valley–dependent exciton densities $n_v(\mathbf{r},t)$ and energies $E_v(\mathbf{r})$, and including the thermalization between exciton populations in different valleys.[236] In this way, it has been predicted that the propagation of KΛ excitons, which have higher occupation than the KK onesin WS_2 monolayers, follows the experimentally observed anti-funneling behavior, cf. Fig. 6(d). Furthermore, the initially faster propagation reflects the larger diffusion coefficients $D(x)$ in the corresponding spatial positions,[236] as the diffusion coefficients depend on strain, i.e., $D \equiv D(s(\mathbf{r}))$, due to opening/closing of intervalley scattering channels.[252] While excitons in WS_2 show an anti-funneling behavior, regular exciton funneling has been observed in $MoSe_2$, where, in contrast to WS_2, most of the exciton population lives in the energetically lower bright KK states.[236]

Similarly, driven by the momentum-dark exciton population, excitons have been found to funnel into dielectric inhomogeneities in WSe_2 bilayers.[275] Furthermore, spin-dark excitons have been recently reported to show the same funneling behavior as KK excitons, i.e., drifting toward regions with high strain.[276] Strain profiles and the resulting funneling can also be engineered by nanoscale tips[274,276,277] and surface acoustic waves.[278,279] In addition, local strain profiles can be used also to create quasi one-dimensional channels, e.g., by depositing the monolayer on top of 1D semiconductor nanowires.[280] This generates a highly anisotropic diffusion with large diffusion coefficients of ≈10 cm^2/s in the direction of the channel at room temperature. These studies exemplify how exciton transport in TMD-based devices can be engineered with strain.[280]

C. Exciton transport in TMD heterostructures

After having discussed transport of excitons in TMD monolayers, we now turn to vertical and lateral heterostructures. Here, the already rich exciton landscape is further extended to spatially separated interlayer excitons, usually denoted as charge transfer (CT) excitons in lateral junctions.

1. Vertical heterostructures

Here, interlayer excitons are composed of electrons and holes residing in different vertically stacked TMD layers and exhibit permanent out-of-plane dipole moments, cf. inset in Fig. 6(e). As a consequence, interlayer excitons display a strong dipole–dipole repulsion, giving rise to a density-dependent renormalization of the exciton energy. Hence, dipole–dipole repulsion becomes manifest in PL spectra as a blue-shift of the exciton resonance at elevated densities.[235,270,281] As expected from Eq. (1), the density-dependent energy renormalization gives rise to a drift force, resulting in a highly anomalous exciton diffusion, where the variance of the spatial distribution of excitons does not evolve linearly in time.[234,235,270,271,282]

In the case of $MoSe_2$-hBN-WSe_2 heterostructures, a superlinear dependence of the spatial variance σ_t^2 with respect to time has been recently observed at exciton densities $n_x > 10^{12}$ cm^{-2},[234] cf. Fig. 6(e). At these high densities, the potential gradient $\nabla V = \nabla(gn)$ is large, and the drift-term in Eq. (1) becomes dominant. Here, g is governed by repulsive dipole–dipole interactions due to the large separation between electrons and holes forming interlayer excitons in this particular heterostructure. Generally, the exciton–exciton interaction consists of two parts—one part stemming from direct dipolar exciton–exciton repulsion and the other part originating from the quantum-mechanical exchange interactions, reflecting the fermionic substructure of excitons.[25,283–285] Importantly, when the separation between the two layers is similar or larger than the exciton Bohr radius, the exchange interaction—which can be negative and thus weaken the exciton–exciton interaction—is suppressed and the direct dipole–dipole repulsion dominates.[286–288] Moreover, the hBN spacer between the TMD layers does not only boost the dipole moment of the interlayer excitons, but it also suppresses the moiré potential, which could trap excitons and affect their propagation in hetero-bilayers.[3,235,289,290]

A recent study on WS_2–WSe_2 bilayers shows that the diffusion of interlayer excitons is highly tunable with the twist angle, which modifies the moiré potential landscape.[3] In particular, the minima of the moiré potential act as traps, hindering the diffusion of excitons and effectively decreasing the diffusion coefficient. Moreover, it has been shown that moiré heterostructures are suitable candidates for realizing Bose–Hubbard models of interlayer excitons, where the twist-angle is used to control both the exciton–exciton interaction strength as well as the inter-site hopping amplitudes.[291,292] These findings indicate that twisted TMD heterostructures could potentially be used as quantum simulators for bosonic many-body systems.

2. Lateral heterostructures

Recently, laterally stacked TMD monolayers have emerged as a promising new platform to study one-dimensional excitons. In these structures, two different monolayers are grown beside each other and covalently stitched together in the plane,[293–299] cf. Fig. 6(f). At the interface, the formation of spatially separated CT excitons has been predicted.[300,301] While for interlayer excitons in vertical heterostructures the spatial separation of electron

and hole is restricted by the layer distance, separations of several nanometers are predicted for CT excitons, thanks to the large device length.[300,301] While exciting far away from the interface leads to the regular monolayer diffusion [black points in top-right Fig. 6(f)], exciting close to the quasi one-dimensional channel formed at the interface results in intriguing transport properties.[300,302–304] The different excitonic energies in the two monolayers drive the propagation of excitons toward and across the interface.[300,302,304] This can be revealed by varying the central position of the excitation spots close to the interface of an hBN-encapsulated $MoSe_2$–WSe_2 lateral heterostucture, showing a non-trivialtemperature depeendence of the diffusion lengthin the two monolayers.[303]

A peculiar spatial expansion along the interface has been observed in a WSe_2–$WS_{1.16}Se_{0.84}$ lateral heterostructure.[300] Here, an abrupt enhancement of the diffusion along the 1D channel is measured for excited densities above 5×10^{12} cm^{-2}, resulting in effective diffusion coefficients of the order of 100 cm^2/s, cf. the red points in Fig. 6(f). This reflects a first-order Mott transition, with the formation of a dense electron–hole plasma that diffuses quickly, leading to a broad electron–hole distribution along the interface already after few tens of picoseconds,[300] cf. bottom row in Fig. 6(f). For intermediate excitation densities (from 1 to 4×10^{12} cm^{-2}), the effective diffusion coefficient increases with the excitation power up to values of few 10 cm^2/s, i.e., up to two orders of magnitude larger than the monolayer values obtained when exciting far away from the interface [cf. Fig. 6(f)]. This increase in the effective diffusion coefficient has been attributed to the dipole–dipole repulsion between CT excitons,[300] favored by the large spatial separations of several nanometers.[301] These results put forward lateral heterojunctions as promising one-dimensional "highways" for excitons and unbound charge-carriers in an electron–hole plasma.

V. OUTLOOK

The vast number of studies on mono- and multi-layered TMDs—highlighting the crucial importance of the rich and versatile exciton landscape for optoelectronic applications and fundamental research—has opened up many avenues that still remain unexplored in this field. Here, we outline some of these prospective research directions.

A. Optics

While optical signatures of the exciton landscape including bright and dark excitons in both TMD monolayers and heterostructures have been extensively studied, the impact of different valley and spin configurations of more complex many-body compounds is still not completely understood. In particular, previous studies have not addressed the potential relevance of trion states with charge carriers located around symmetry points other than the K or K′ valleys. Although it is well known that excitons formed by electrons (holes) at the Λ (Γ) point are the energetically lowest or very close to the lowest-lying states in some monolayers and heterostructures,[42,102,258] the energetic position of, e.g., trion or biexciton states composed of charges in these valleys has remained in the dark. The optical response of these higher-order charge complexes could be further controlled by tuning the relative energetic position of the involved valleys with strain.[257,258]

The impact of strongly correlated states on the optical response of TMDs is a hot topic of research that still needs to be further explored. Very recently, signatures of many-body states beyond trions have been identified in reflectance spectra of heavily electron-doped WSe_2 monolayers.[305] While these signatures have been proposed to arise from six- and eight-body exciton states interacting with the Fermi sea of doping charges,[306] it remains unclear why these many-body compounds are not experimentally observed in hole-doped samples. The optical fingerprint of excitons interacting with a Wigner crystal of electrons has also been reported,[307] providing a tool to investigate strongly correlated electron systems. A recent theoretical study has suggested using terahertz light to directly probe the internal quantum transitions of the Wigner crystal itself.[308] The experimental realization of correlated exciton phases such as exciton Wigner supersolids[309,310] could shed light on the interplay between exciton–exciton interactions and their bosonic quantum statistics.

Regarding TMD polaritonics, one current focus in this field concerns utilizing polaritons as both a probe of, and as a potential means to control microscopic processes in TMDs. For example, recent theoretical studies have explored how the shape of the polariton dispersion and modification of the effective phonon scattering matrix can drastically alter phonon scattering rates in comparison to bare excitons.[311,312] Even more sophisticated microscopic theories will be necessary to fully describe newly reported hybrid exciton–photon–phonon states.[313] Moving beyond monolayer exciton–polaritons provides a promising route toward quantum nonlinear devices. In addition to trion polaritons,[162] interlayer exciton–polaritons represent an exciting combination of quantum tunneling with strong light–matter coupling that possesses a permanent dipole moment.[314,315] These dipolaritons offer enhanced nonlinearity, as well as highly controllable polariton transport and condensation, making them relevant for potential quantum optoelectronic applications.[316]

B. Dynamics

The recent observation of the ultrafast formation of momentum-dark excitons in tr-ARPES measurements[53] represents a major step forward in the characterization and understanding of the exciton dynamics in TMD monolayers and heterostructures. Nevertheless, these recent experiments excited the TMD with linearly polarized light and, therefore, simultaneously generated KK and K′K′ excitons with opposite spin configurations. Therefore, the spin-relaxation via, e.g., scattering with chiral phonons or intervalley exchange could not be distinguished from spin-conserving intervalley thermalization. The direct visualization and understanding of the main spin relaxation processes would be crucial for an accurate characterization of the limits and advantages of TMD-based spintronic devices.

Moreover, the first tr-ARPES studies on TMD heterostructures have been performed revealing crucial insights into the main charge transfer channels,[56] as well as indications of exciton localization resulting from superlattice-periodic moiré potential.[104] However, further studies of this kind involving different hetero-/homo-bilayers and varying crucial system parameters such

as twist-angle and temperature are necessary to confirm these first observations and to provide conclusive understanding of charge-transfer and localization dynamics. In particular, resolving the small moiré induced splittings of the ARPES signal in momentum and energy and preparing comparable samples with different stacking configurations provides a major experimental challenge. Furthermore, a microscopic model predicting the ARPES signatures of strongly correlated electronic states, as well as superlattice Umklapp-processes, is still missing.

Exciton–exciton annihilation in TMD monolayers has been well characterized so far—the main scattering channels involved have been identified[196] and the tunability with external knobs has been explored.[187,195–197] However, the understanding of Auger recombination of excitons in TMD heterostructures is still lacking. While it has been observed that EEA is severely weakened in homobilayers,[192] the microscopic origin of this suppression is unclear. More experimental and theoretical studies are needed to understand the microscopic mechanisms behind EEA and the tunability of this process in TMD heterostructures.

Studies on excitonic many-body complexes have so far focused on the optical fingerprint of these quasi-particles in absorption and PL spectra. Only recently the trion thermalization dynamics have been investigated by exploiting the temporal evolution of the PL line shape.[207] Similar methods could be used to study the thermalization dynamics of other many-body complexes such as polaritons and biexcitons. Such experimental studies, together with appropriate theoretical models, would provide a better understanding of the main scattering mechanisms involved in the thermalization of photoexcited charges. The latter is crucial for an optimal design of efficient optoelectronic devices.

C. Transport

In recent years, the intrinsic mechanisms governing exciton diffusion and funneling have been well established. In particular, exciton diffusion is known to be controlled by exciton–phonon scattering at low exciton densities[233] and to be hindered by dielectric inhomogeneities and traps.[14] It has also been understood that KK and KΛ excitons funnel in opposite directions of the strain gradient, although the reason for the unexpectedly large optical activation of KΛ excitons at room temperature has remained unclear.[236] Furthermore, the understanding of the mechanisms governing the transport of more complex many-particle compounds is still lacking. The few reported diffusion coefficients for, e.g., trions, differ substantially in the current literature,[237,245,253,261] indicating the difficulty in accurately assessing the transport properties of many-particle states. Future studies should aim to thoroughly characterize diffusion of trions and other many-particle compounds consistently across different samples, temperatures, doping levels, and excitation densities in order to gain a better understanding of the underlying microscopic mechanisms. We anticipate that, not only the main scattering mechanisms hindering propagation should be identified, but also the interplay between different many-particle compounds that might coexist (e.g., trions, excitons and single electrons) should be better understood. While research on excitons and higher-order charge complexes in atomically thin materials has significantly advanced in the last decade, there is still a lot of new and exciting physics to be explored in the coming years.

ACKNOWLEDGMENTS

We acknowledge funding from the Deutsche Forschungsgemeinschaft (DFG) via Grant No. SFB 1083 and the European Union's Horizon 2020 research and innovation funding program under Grant Agreement No. 881603 (Graphene Flagship). R.P.-C. acknowledges funding from the Excellence Initiative Nano (Chalmers University of Technology) under its Excellence Ph.D. program.

AUTHOR DECLARATIONS

Conflict of Interest

The authors have no conflicts to disclose.

Author Contributions

R.P.-C and D.E contributed equally to this work

Raul Perea-Causin: Conceptualization (equal); Investigation (equal); Resources (equal); Visualization (equal); Writing – original draft (lead); Writing – review & editing (lead). **Daniel Erkensten**: Conceptualization (equal); Investigation (equal); Resources (equal); Visualization (equal); Writing – original draft (lead); Writing – review & editing (lead). **Jamie M. Fitzgerald**: Conceptualization (equal); Investigation (equal); Resources (equal); Visualization (equal); Writing – original draft (equal); Writing – review & editing (equal). **Joshua J. P. Thompson**: Conceptualization (equal); Investigation (equal); Resources (equal); Visualization (equal); Writing – original draft (equal); Writing – review & editing (equal). **Roberto Rosati**: Conceptualization (equal); Investigation (equal); Resources (equal); Visualization (equal); Writing – original draft (equal). **Samuel Brem**: Conceptualization (equal); Investigation (equal); Resources (equal); Visualization (equal); Writing – original draft (equal). **Ermin Malic**: Conceptualization (lead); Funding acquisition (equal); Investigation (equal); Project administration (lead); Resources (equal); Visualization (equal); Writing – original draft (equal); Writing – review & editing (equal).

DATA AVAILABILITY

Data sharing is not applicable to this article as no new data were created or analyzed in this study.

REFERENCES

[1] G. Wang, A. Chernikov, M. M. Glazov, T. F. Heinz, X. Marie, T. Amand, and B. Urbaszek, "Colloquium: Excitons in atomically thin transition metal dichalcogenides," Rev. Mod. Phys. **90**, 021001 (2018).
[2] T. Mueller and E. Malic, "Exciton physics and device application of two-dimensional transition metal dichalcogenide semiconductors," npj 2D Mater. Appl. **2**, 29 (2018).
[3] D. Huang, J. Choi, C.-K. Shih, and X. Li, "Excitons in semiconductor moiré superlattices," Nat. Nanotechnol. **17**, 227 (2022).
[4] A. Ciarrocchi, F. Tagarelli, A. Avsar, and A. Kis, "Excitonic devices with van der Waals heterostructures: Valleytronics meets twistronics," Nat. Rev. Mater. **7**, 449–464 (2022).

[5]E. C. Regan, D. Wang, E. Y. Paik, Y. Zeng, L. Zhang, J. Zhu, A. H. MacDonald, H. Deng, and F. Wang, "Emerging exciton physics in transition metal dichalcogenide heterobilayers," Nat. Rev. Mater. **7**, 778 (2022).
[6]K. S. Novoselov, A. Mishchenko, A. Carvalho, and A. H. Castro Neto, "2D materials and van der Waals heterostructures," Science **353**, aac9439 (2016).
[7]A. Chernikov, T. C. Berkelbach, H. M. Hill, A. Rigosi, Y. Li, O. B. Aslan, D. R. Reichman, M. S. Hybertsen, and T. F. Heinz, "Exciton binding energy and nonhydrogenic Rydberg series in monolayer WS_2," Phys. Rev. Lett. **113**, 076802 (2014).
[8]H. Yu, X. Cui, X. Xu, and W. Yao, "Valley excitons in two-dimensional semiconductors," Natl. Sci. Rev. **2**, 57–70 (2015).
[9]E. Malic, M. Selig, M. Feierabend, S. Brem, D. Christiansen, F. Wendler, A. Knorr, and G. Berghäuser, "Dark excitons in transition metal dichalcogenides," Phys. Rev. Mater. **2**, 014002 (2018).
[10]P. Rivera, J. R. Schaibley, A. M. Jones, J. S. Ross, S. Wu, G. Aivazian, P. Klement, K. Seyler, G. Clark, N. J. Ghimire, J. Yan, D. G. Mandrus, W. Yao, and X. Xu, "Observation of long-lived interlayer excitons in monolayer $MoSe_2$–WSe_2 heterostructures," Nat. Commun. **6**, 6242 (2015).
[11]K. F. Mak, C. Lee, J. Hone, J. Shan, and T. F. Heinz, "Atomically thin MoS_2: A new direct-gap semiconductor," Phys. Rev. Lett. **105**, 136805 (2010).
[12]A. Splendiani, L. Sun, Y. Zhang, T. Li, J. Kim, C.-Y. Chim, G. Galli, and F. Wang, "Emerging photoluminescence in monolayer MoS_2," Nano Lett. **10**, 1271–1275 (2010).
[13]Y. Uchiyama, A. Kutana, K. Watanabe, T. Taniguchi, K. Kojima, T. Endo, Y. Miyata, H. Shinohara, and R. Kitaura, "Momentum-forbidden dark excitons in hBN-encapsulated monolayer MoS_2," npj 2D Mater. Appl. **3**, 26 (2019).
[14]A. Raja, L. Waldecker, J. Zipfel, Y. Cho, S. Brem, J. D. Ziegler, M. Kulig, T. Taniguchi, K. Watanabe, E. Malic, T. F. Heinz, T. C. Berkelbach, and A. Chernikov, "Dielectric disorder in two-dimensional materials," Nat. Nanotechnol. **14**, 832–837 (2019).
[15]C. R. Dean, A. F. Young, I. Meric, C. Lee, L. Wang, S. Sorgenfrei, K. Watanabe, T. Taniguchi, P. Kim, K. L. Shepard, and J. Hone, "Boron nitride substrates for high-quality graphene electronics," Nat. Nanotechnol. **5**, 722–726 (2010).
[16]Z. Ye, L. Waldecker, E. Y. Ma, D. Rhodes, A. Antony, B. Kim, X.-X. Zhang, M. Deng, Y. Jiang, Z. Lu, D. Smirnov, K. Watanabe, T. Taniguchi, J. Hone, and T. F. Heinz, "Efficient generation of neutral and charged biexcitons in encapsulated WSe_2 monolayers," Nat. Commun. **9**, 3718 (2018).
[17]K. F. Mak, K. He, J. Shan, and T. F. Heinz, "Control of valley polarization in monolayer MoS_2 by optical helicity," Nat. Nanotechnol. **7**, 494–498 (2012).
[18]M. Goryca, J. Li, A. V. Stier, T. Taniguchi, K. Watanabe, E. Courtade, S. Shree, C. Robert, B. Urbaszek, X. Marie, and S. A. Crooker, "Revealing exciton masses and dielectric properties of monolayer semiconductors with high magnetic fields," Nat. Commun. **10**, 4172 (2019).
[19]G. Berghäuser, A. Knorr, and E. Malic, "Optical fingerprint of dark 2p-states in transition metal dichalcogenides," 2D Mater. **4**, 015029 (2016).
[20]M. Selig, G. Berghäuser, A. Raja, P. Nagler, C. Schüller, T. F. Heinz, T. Korn, A. Chernikov, E. Malic, and A. Knorr, "Excitonic linewidth and coherence lifetime in monolayer transition metal dichalcogenides," Nat. Commun. **7**, 13279 (2016).
[21]G. Gupta and K. Majumdar, "Fundamental exciton linewidth broadening in monolayer transition metal dichalcogenides," Phys. Rev. B **99**, 085412 (2019).
[22]S. Brem, J. Zipfel, M. Selig, A. Raja, L. Waldecker, J. D. Ziegler, T. Taniguchi, K. Watanabe, A. Chernikov, and E. Malic, "Intrinsic lifetime of higher excitonic states in tungsten diselenide monolayers," Nanoscale **11**, 12381–12387 (2019).
[23]J. Fang, K. Yao, T. Zhang, M. Wang, T. Jiang, S. Huang, B. A. Korgel, M. Terrones, A. Alù, and Y. Zheng, "Room-temperature observation of near-intrinsic exciton linewidth in monolayer WS_2," Adv. Mater. **34**, 2108721 (2022).
[24]F. Katsch, M. Selig, and A. Knorr, "Exciton-scattering-induced dephasing in two-dimensional semiconductors," Phys. Rev. Lett. **124**, 257402 (2020).
[25]D. Erkensten, S. Brem, and E. Malic, "Exciton-exciton interaction in transition metal dichalcogenide monolayers and van der Waals heterostructures," Phys. Rev. B **103**, 045426 (2021).
[26]Maja Feierabend, Alexandre Morlet, Gunnar Berghäuser, and Ermin Malic, "Impact of strain on the optical fingerprint of monolayer transition-metal dichalcogenides," Phys. Rev. B **96**, 045425 (2017).
[27]W. Yao, D. Xiao, and Q. Niu, "Valley-dependent optoelectronics from inversion symmetry breaking," Phys. Rev. B **77**, 235406 (2008).
[28]D. Xiao, G.-B. Liu, W. Feng, X. Xu, and W. Yao, "Coupled spin and valley physics in monolayers of MoS_2 and other group-VI dichalcogenides," Phys. Rev. Lett. **108**, 196802 (2012).
[29]H. Zeng, J. Dai, W. Yao, D. Xiao, and X. Cui, "Valley polarization in MoS_2 monolayers by optical pumping," Nat. Nanotechnol. **7**, 490–493 (2012).
[30]J. Lee, K. F. Mak, and J. Shan, "Electrical control of the valley Hall effect in bilayer MoS_2 transistors," Nat. Nanotechnol. **11**, 421–425 (2016).
[31]J. R. Schaibley, H. Yu, G. Clark, P. Rivera, J. S. Ross, K. L. Seyler, W. Yao, and X. Xu, "Valleytronics in 2D materials," Nat. Rev. Mater. **1**, 16055 (2016).
[32]X. Lu, X. Chen, S. Dubey, Q. Yao, W. Li, X. Wang, Q. Xiong, and A. Srivastava, "Optical initialization of a single spin-valley in charged WSe_2 quantum dots," Nat. Nanotechnol. **14**, 426–431 (2019).
[33]Z. Gong, G. B. Liu, H. Yu, D. Xiao, X. Cui, X. Xu, and W. Yao, "Magnetoelectric effects and valley-controlled spin quantum gates in transition metal dichalcogenide bilayers," Nat. Commun. **4**, 2053 (2013).
[34]H. Rostami and R. Asgari, "Valley Zeeman effect and spin-valley polarized conductance in monolayer MoS_2 in a perpendicular magnetic field," Phys. Rev. B **91**, 075433 (2015).
[35]M. Eginligil, B. Cao, Z. Wang, X. Shen, C. Cong, J. Shang, C. Soci, and T. Yu, "Dichroic spin–valley photocurrent in monolayer molybdenum disulphide," Nat. Commun. **6**, 7636 (2015).
[36]M. Palummo, M. Bernardi, and J. C. Grossman, "Exciton radiative lifetimes in two-dimensional transition metal dichalcogenides," Nano Lett. **15**, 2794–2800 (2015).
[37]S. Brem, M. Selig, G. Berghaeuser, and E. Malic, "Exciton relaxation cascade in two-dimensional transition metal dichalcogenides," Sci. Rep. **8**, 8238 (2018).
[38]C. Trovatello, F. Katsch, N. J. Borys, M. Selig, K. Yao, R. Borrego-Varillas, F. Scotognella, I. Kriegel, A. Yan, A. Zettl *et al.*, "The ultrafast onset of exciton formation in 2D semiconductors," Nat. Commun. **11**, 5277 (2020).
[39]S. Brem, A. Ekman, D. Christiansen, F. Katsch, M. Selig, C. Robert, X. Marie, B. Urbaszek, A. Knorr, and E. Malic, "Phonon-assisted photoluminescence from indirect excitons in monolayers of transition-metal dichalcogenides," Nano Lett. **20**, 2849–2856 (2020).
[40]J. Lindlau, M. Selig, A. Neumann, L. Colombier, J. Förste, V. Funk, M. Förg, J. Kim, G. Berghäuser, T. Taniguchi *et al.*, "The role of momentum-dark excitons in the elementary optical response of bilayer WSe_2," Nat. Commun. **9**, 2586 (2018).
[41]X.-X. Zhang, Y. You, S. Y. F. Zhao, and T. F. Heinz, "Experimental evidence for dark excitons in monolayer WSe_2," Phys. Rev. Lett. **115**, 257403 (2015).
[42]T. Deilmann and K. S. Thygesen, "Finite-momentum exciton landscape in mono- and bilayer transition metal dichalcogenides," 2D Mater. **6**, 035003 (2019).
[43]Z. Li, T. Wang, C. Jin, Z. Lu, Z. Lian, Y. Meng, M. Blei, S. Gao, T. Taniguchi, K. Watanabe, T. Ren, S. Tongay, L. Yang, D. Smirnov, T. Cao, and S.-F. Shi, "Emerging photoluminescence from the dark-exciton phonon replica in monolayer WSe_2," Nat. Commun. **10**, 2469 (2019).
[44]J. Lindlau, C. Robert, V. Funk, J. Förste, M. Förg, L. Colombier, A. Neumann, E. Courtade, S. Shree, T. Taniguchi *et al.*, "Identifying optical signatures of momentum-dark excitons in transition metal dichalcogenide monolayers," arXiv:1710.00988 (2017).
[45]V. Funk, K. Wagner, E. Wietek, J. D. Ziegler, J. Förste, J. Lindlau, M. Förg, K. Watanabe, T. Taniguchi, A. Chernikov, and A. Högele, "Spectral asymmetry of phonon sideband luminescence in monolayer and bilayer WSe_2," Phys. Rev. Res. **3**, L042019 (2021).
[46]M. He, P. Rivera, D. Van Tuan, N. P. Wilson, M. Yang, T. Taniguchi, K. Watanabe, J. Yan, D. G. Mandrus, H. Yu, H. Dery, W. Yao, and X. Xu, "Valley phonons and exciton complexes in a monolayer semiconductor," Nat. Commun. **11**, 618 (2020).
[47]E. Liu, J. van Baren, C.-T. Liang, T. Taniguchi, K. Watanabe, N. M. Gabor, Y.-C. Chang, and C. H. Lui, "Multipath optical recombination of intervalley dark excitons and trions in monolayer WSe_2," Phys. Rev. Lett. **124**, 196802 (2020).
[48]D. Christiansen, M. Selig, G. Berghäuser, R. Schmidt, I. Niehues, R. Schneider, A. Arora, S. M. de Vasconcellos, R. Bratschitsch, E. Malic, and A. Knorr, "Phonon sidebands in monolayer transition metal dichalcogenides," Phys. Rev. Lett. **119**, 187402 (2017).

[49]C. Robert, T. Amand, F. Cadiz, D. Lagarde, E. Courtade, M. Manca, T. Taniguchi, K. Watanabe, B. Urbaszek, and X. Marie, "Fine structure and lifetime of dark excitons in transition metal dichalcogenide monolayers," Phys. Rev. B **96**, 155423 (2017).
[50]G.-H. Peng, P.-Y. Lo, W.-H. Li, Y.-C. Huang, Y.-H. Chen, C.-H. Lee, C.-K. Yang, and S.-J. Cheng, "Distinctive signatures of the spin- and momentum-forbidden dark exciton states in the photoluminescence of strained WSe_2 monolayers under thermalization," Nano Lett. **19**, 2299–2312 (2019).
[51]M. Feierabend, S. Brem, A. Ekman, and E. Malic, "Brightening of spin- and momentum-dark excitons in transition metal dichalcogenides," 2D Mater. **8**, 015013 (2021).
[52]G. Wang, C. Robert, M. M. Glazov, F. Cadiz, E. Courtade, T. Amand, D. Lagarde, T. Taniguchi, K. Watanabe, B. Urbaszek, and X. Marie, "In-plane propagation of light in transition metal dichalcogenide monolayers: Optical selection rules," Phys. Rev. Lett. **119**, 047401 (2017).
[53]J. Madéo, M. K. L. Man, C. Sahoo, M. Campbell, V. Pareek, E. L. Wong, A. Al-Mahboob, N. S. Chan, A. Karmakar, B. M. K. Mariserla, X. Li, T. F. Heinz, T. Cao, and K. M. Dani, "Directly visualizing the momentum-forbidden dark excitons and their dynamics in atomically thin semiconductors," Science **370**, 1199–1204 (2020).
[54]W. Lee, Y. Lin, L.-S. Lu, W.-C. Chueh, M. Liu, X. Li, W.-H. Chang, R. A. Kaindl, and C.-K. Shih, "Time-resolved ARPES determination of a quasi-particle band gap and hot electron dynamics in monolayer MoS_2," Nano Lett. **21**, 7363–7370 (2021).
[55]R. Wallauer, R. Perea-Causin, L. Münster, S. Zajusch, S. Brem, J. Güdde, K. Tanimura, K.-Q. Lin, R. Huber, E. Malic, and U. Höfer, "Momentum-resolved observation of exciton formation dynamics in monolayer WS_2," Nano Lett. **21**, 5867–5873 (2021).
[56]D. Schmitt, J. P. Bange, W. Bennecke, A. AlMutairi, G. Meneghini, K. Watanabe, T. Taniguchi, D. Steil, D. R. Luke, R. T. Weitz *et al.*, "Formation of moiré interlayer excitons in space and time," Nature **608**, 499–503 (2022).
[57]S. Dong, M. Puppin, T. Pincelli, S. Beaulieu, D. Christiansen, H. Hübener, C. W. Nicholson, R. P. Xian, M. Dendzik, Y. Deng, Y. W. Windsor, M. Selig, E. Malic, A. Rubio, A. Knorr, M. Wolf, L. Rettig, and R. Ernstorfer, "Direct measurement of key exciton properties: Energy, dynamics, and spatial distribution of the wave function," Nat. Sci. **1**, e10010 (2021).
[58]K. F. Mak, K. He, C. Lee, G. H. Lee, J. Hone, T. F. Heinz, and J. Shan, "Tightly bound trions in monolayer MoS_2," Nat. Mater. **12**, 207–211 (2013).
[59]J. S. Ross, S. Wu, H. Yu, N. J. Ghimire, A. M. Jones, G. Aivazian, J. Yan, D. G. Mandrus, D. Xiao, W. Yao, and X. Xu, "Electrical control of neutral and charged excitons in a monolayer semiconductor," Nat. Commun. **4**, 1474 (2013).
[60]G. Plechinger, P. Nagler, A. Arora, R. Schmidt, A. Chernikov, A. G. Del Águila, P. C. Christianen, R. Bratschitsch, C. Schüller, and T. Korn, "Trion fine structure and coupled spin–valley dynamics in monolayer tungsten disulfide," Nat. Commun. **7**, 12715 (2016).
[61]E. Courtade, M. Semina, M. Manca, M. M. Glazov, C. Robert, F. Cadiz, G. Wang, T. Taniguchi, K. Watanabe, M. Pierre, W. Escoffier, E. L. Ivchenko, P. Renucci, X. Marie, T. Amand, and B. Urbaszek, "Charged excitons in monolayer WSe_2: Experiment and theory," Phys. Rev. B **96**, 085302 (2017).
[62]M. Sidler, P. Back, O. Cotlet, A. Srivastava, T. Fink, M. Kroner, E. Demler, and A. Imamoglu, "Fermi polaron-polaritons in charge-tunable atomically thin semiconductors," Nat. Phys. **13**, 255–261 (2017).
[63]K. Hao, J. F. Specht, P. Nagler, L. Xu, K. Tran, A. Singh, C. K. Dass, C. Schüller, T. Korn, M. Richter, A. Knorr, X. Li, and G. Moody, "Neutral and charged inter-valley biexcitons in monolayer $MoSe_2$," Nat. Commun. **8**, 15552 (2017).
[64]A. Steinhoff, M. Florian, A. Singh, K. Tran, M. Kolarczik, S. Helmrich, A. W. Achtstein, U. Woggon, N. Owschimikow, F. Jahnke, and X. Li, "Biexciton fine structure in monolayer transition metal dichalcogenides," Nat. Phys. **14**, 1199–1204 (2018).
[65]F. Katsch and A. Knorr, "Optical preparation and coherent control of ultrafast nonlinear quantum superpositions in exciton gases: A case study for atomically thin semiconductors," Phys. Rev. X **10**, 041039 (2020).
[66]Z. Li, T. Wang, Z. Lu, C. Jin, Y. Chen, Y. Meng, Z. Lian, T. Taniguchi, K. Watanabe, S. Zhang *et al.*, "Revealing the biexciton and trion-exciton complexes in bn encapsulated WSe_2," Nat. Commun. **9**, 3719 (2018).
[67]M. Barbone, A. R.-P. Montblanch, D. M. Kara, C. Palacios-Berraquero, A. R. Cadore, D. De Fazio, B. Pingault, E. Mostaani, H. Li, B. Chen, K. Watanabe, T. Taniguchi, S. Tongay, G. Wang, A. C. Ferrari, and M. Atatüre, "Charge-tuneable biexciton complexes in monolayer WSe_2," Nat. Commun. **9**, 3721 (2018).
[68]M. Paur, A. J. Molina-Mendoza, R. Bratschitsch, K. Watanabe, T. Taniguchi, and T. Mueller, "Electroluminescence from multi-particle exciton complexes in transition metal dichalcogenide semiconductors," Nat. Commun. **10**, 1709 (2019).
[69]Y. V. Zhumagulov, A. Vagov, D. R. Gulevich, P. E. Faria Junior, and V. Perebeinos, "Trion induced photoluminescence of a doped MoS_2 monolayer," Chem. Phys. **153**, 044132 (2020).
[70]P. Rivera, M. He, B. Kim, S. Liu, C. Rubio-Verdú, H. Moon, L. Mennel, D. A. Rhodes, H. Yu, T. Taniguchi *et al.*, "Intrinsic donor-bound excitons in ultraclean monolayer semiconductors," Nat. Commun. **12**, 871 (2021).
[71]R. A. Suris, V. P. Kochereshko, G. V. Astakhov, D. R. Yakovlev, W. Ossau, J. Nürnberger, W. Faschinger, G. Landwehr, T. Wojtowicz, G. Karczewski, and J. Kossut, "Excitons and trions modified by interaction with a two-dimensional electron gas," Phys. Status Solidi B **227**, 343–352 (2001).
[72]D. K. Efimkin and A. H. MacDonald, "Many-body theory of trion absorption features in two-dimensional semiconductors," Phys. Rev. B **95**, 035417 (2017).
[73]E. Liu, J. van Baren, Z. Lu, M. M. Altaiary, T. Taniguchi, K. Watanabe, D. Smirnov, and C. H. Lui, "Gate tunable dark trions in monolayer WSe_2," Phys. Rev. Lett. **123**, 027401 (2019).
[74]S. Tongay, J. Suh, C. Ataca, W. Fan, A. Luce, J. S. Kang, J. Liu, C. Ko, R. Raghunathanan, J. Zhou *et al.*, "Defects activated photoluminescence in two-dimensional semiconductors: Interplay between bound, charged and free excitons," Sci. Rep. **3**, 2657 (2013).
[75]P. Tonndorf, R. Schmidt, R. Schneider, J. Kern, M. Buscema, G. A. Steele, A. Castellanos-Gomez, H. S. J. van der Zant, S. Michaelis de Vasconcellos, and R. Bratschitsch, "Single-photon emission from localized excitons in an atomically thin semiconductor," Optica **2**, 347–352 (2015).
[76]J. He, D. He, Y. Wang, Q. Cui, F. Ceballos, and H. Zhao, "Spatiotemporal dynamics of excitons in monolayer and bulk WS_2," Nanoscale **7**, 9526 (2015).
[77]J. J. P. Thompson, S. Brem, H. Fang, J. Frey, S. P. Dash, W. Wieczorek, and E. Malic, "Criteria for deterministic single-photon emission in two-dimensional atomic crystals," Phys. Rev. Mater. **4**, 084006 (2020).
[78]K. Parto, S. I. Azzam, K. Banerjee, and G. Moody, "Defect and strain engineering of monolayer WSe_2 enables site-controlled single-photon emission up to 150 K," Nat. Commun. **12**, 3585 (2021).
[79]A. Arora, T. Deilmann, T. Reichenauer, J. Kern, S. Michaelis de Vasconcellos, M. Rohlfing, and R. Bratschitsch, "Excited-state trions in monolayer WS_2," Phys. Rev. Lett. **123**, 167401 (2019).
[80]K. Wagner, E. Wietek, J. D. Ziegler, M. A. Semina, T. Taniguchi, K. Watanabe, J. Zipfel, M. M. Glazov, and A. Chernikov, "Autoionization and dressing of excited excitons by free carriers in monolayer WSe_2," Phys. Rev. Lett. **125**, 267401 (2020).
[81]E. Liu, J. van Baren, Z. Lu, T. Taniguchi, K. Watanabe, D. Smirnov, Y.-C. Chang, and C. H. Lui, "Exciton-polaron Rydberg states in monolayer $MoSe_2$ and WSe_2," Nat. Commun. **12**, 6131 (2021).
[82]D. A. Ruiz-Tijerina, M. Danovich, C. Yelgel, V. Zólyomi, and V. I. Fal'ko, "Hybrid k·p tight-binding model for subbands and infrared intersubband optics in few-layer films of transition-metal dichalcogenides: MoS_2, $MoSe_2$, WS_2, and WSe_2," Phys. Rev. B **98**, 035411 (2018).
[83]T. Chu, H. Ilatikhameneh, G. Klimeck, R. Rahman, and Z. Chen, "Electrically tunable bandgaps in bilayer MoS_2," Nano Lett. **15**, 8000–8007 (2015).
[84]H. J. Conley, B. Wang, J. I. Ziegler, R. F. Haglund, S. T. Pantelides, and K. I. Bolotin, "Bandgap engineering of strained monolayer and bilayer MoS_2," Nano Lett. **13**, 3626–3630 (2013).
[85]N. Leisgang, S. Shree, I. Paradisanos, L. Sponfeldner, C. Robert, D. Lagarde, A. Balocchi, K. Watanabe, T. Taniguchi, X. Marie *et al.*, "Giant Stark splitting of an exciton in bilayer MoS_2," Nat. Nanotechnol. **15**, 901–907 (2020).
[86]B. Miller, A. Steinhoff, B. Pano, J. Klein, F. Jahnke, A. Holleitner, and U. Wurstbauer, "Long-lived direct and indirect interlayer excitons in van der Waals heterostructures," Nano Lett. **17**, 5229–5237 (2017).
[87]C. Jiang, W. Xu, A. Rasmita, Z. Huang, K. Li, Q. Xiong, and W.-b. Gao, "Microsecond dark-exciton valley polarization memory in two-dimensional heterostructures," Nat. Commun. **9**, 753 (2018).

[88]Z. Huang, Y. Liu, K. Dini, Q. Tan, Z. Liu, H. Fang, J. Liu, T. Liew, and W. Gao, "Robust room temperature valley Hall effect of interlayer excitons," Nano Lett. **20**, 1345–1351 (2019).
[89]M. M. Furchi, F. Höller, L. Dobusch, D. K. Polyushkin, S. Schuler, and T. Mueller, "Device physics of van der Waals heterojunction solar cells," npj 2D Mater. Appl. **2**, 3 (2018).
[90]L. A. Jauregui, A. Y. Joe, K. Pistunova, D. S. Wild, A. A. High, Y. Zhou, G. Scuri, K. De Greve, A. Sushko, C.-H. Yu *et al.*, "Electrical control of interlayer exciton dynamics in atomically thin heterostructures," Science **366**, 870–875 (2019).
[91]J. Kiemle, F. Sigger, M. Lorke, B. Miller, K. Watanabe, T. Taniguchi, A. Holleitner, and U. Wurstbauer, "Control of the orbital character of indirect excitons in MoS_2/WS_2 heterobilayers," Phys. Rev. B **101**, 121404 (2020).
[92]A. Ciarrocchi, D. Unuchek, A. Avsar, K. Watanabe, T. Taniguchi, and A. Kis, "Polarization switching and electrical control of interlayer excitons in two-dimensional van der Waals heterostructures," Nat. Photonics **13**, 131–136 (2019).
[93]T. Deilmann and K. S. Thygesen, "Interlayer excitons with large optical amplitudes in layered van der Waals materials," Nano Lett. **18**, 2984–2989 (2018).
[94]N. Peimyoo, T. Deilmann, F. Withers, J. Escolar, D. Nutting, T. Taniguchi, K. Watanabe, A. Taghizadeh, M. F. Craciun, K. S. Thygesen, and S. Russo, "Electrical tuning of optically active interlayer excitons in bilayer MoS_2," Nat. Nanotechnol. **16**, 888–893 (2021).
[95]H. Yu, G.-B. Liu, J. Tang, X. Xu, and W. Yao, "Moiré excitons: From programmable quantum emitter arrays to spin-orbit–coupled artificial lattices," Sci. Adv. **3**, e1701696 (2017).
[96]P. Rivera, H. Yu, K. L. Seyler, N. P. Wilson, W. Yao, and X. Xu, "Interlayer valley excitons in heterobilayers of transition metal dichalcogenides," Nat. Nanotechnol. **13**, 1004–1015 (2018).
[97]K. L. Seyler, P. Rivera, H. Yu, N. P. Wilson, E. L. Ray, D. G. Mandrus, J. Yan, W. Yao, and X. Xu, "Signatures of moiré-trapped valley excitons in $MoSe_2/WSe_2$ heterobilayers," Nature **567**, 66–70 (2019).
[98]K. Tran, G. Moody, F. Wu, X. Lu, J. Choi, K. Kim, A. Rai, D. A. Sanchez, J. Quan, A. Singh, J. Embley, A. Zepeda, M. Campbell, T. Autry, T. Taniguchi, K. Watanabe, N. Lu, S. K. Banerjee, K. L. Silverman, S. Kim, E. Tutuc, L. Yang, A. H. MacDonald, and X. Li, "Evidence for moiré excitons in van der Waals heterostructures," Nature **567**, 71–75 (2019).
[99]F. Wu, T. Lovorn, and A. MacDonald, "Theory of optical absorption by interlayer excitons in transition metal dichalcogenide heterobilayers," Phys. Rev. B **97**, 035306 (2018).
[100]D. A. Ruiz-Tijerina and V. I. Fal'ko, "Interlayer hybridization and moiré superlattice minibands for electrons and excitons in heterobilayers of transition-metal dichalcogenides," Phys. Rev. B **99**, 125424 (2019).
[101]S. Brem, C. Linderälv, P. Erhart, and E. Malic, "Tunable phases of moiré excitons in van der Waals heterostructures," Nano Lett. **20**, 8534 (2020).
[102]J. Hagel, S. Brem, C. Linderälv, P. Erhart, and E. Malic, "Exciton landscape in van der Waals heterostructures," Phys. Rev. Res. **3**, 043217 (2021).
[103]N. Zhang, A. Surrente, M. Baranowski, D. K. Maude, P. Gant, A. Castellanos-Gomez, and P. Plochocka, "Moiré intralayer excitons in a $MoSe_2/MoS_2$ heterostructure," Nano Lett. **18**, 7651–7657 (2018).
[104]O. Karni, E. Barré, V. Pareek, J. D. Georgaras, M. K. L. Man, C. Sahoo, D. R. Bacon, X. Zhu, H. B. Ribeiro A. L. O'Beirne *et al.*, "Structure of the moiré exciton captured by imaging its electron and hole," Nature **603**, 247–252 (2022).
[105]M. R. Rosenberger, H.-J. Chuang, M. Phillips, V. P. Oleshko, K. M. McCreary, S. V. Sivaram, C. S. Hellberg, and B. T. Jonker, "Twist angle-dependent atomic reconstruction and moiré patterns in transition metal dichalcogenide heterostructures," ACS Nano **14**, 4550–4558 (2020).
[106]T. I. Andersen, G. Scuri, A. Sushko, K. De Greve, J. Sung, Y. Zhou, D. S. Wild, R. J. Gelly, H. Heo, D. Bérubé *et al.*, "Excitons in a reconstructed moiré potential in twisted WSe_2/WSe_2 homobilayers," Nat. Mater. **20**, 480–487 (2021).
[107]V. V. Enaldiev, F. Ferreira, S. J. Magorrian, and V. I. Fal'ko, "Piezoelectric networks and ferroelectric domains in twistronic superlattices in WS_2/MoS_2 and $WSe_2/MoSe_2$ bilayers," 2D Mater. **8**, 025030 (2021).
[108]D. Edelberg, H. Kumar, V. Shenoy, H. Ochoa, and A. N. Pasupathy, "Tunable strain soliton networks confine electrons in van der Waals materials," Nat. Phys. **16**, 1097–1102 (2020).
[109]M. Brotons-Gisbert, H. Baek, A. Campbell, K. Watanabe, T. Taniguchi, and B. D. Gerardot, "Moiré-trapped interlayer trions in a charge-tunable $WSe_2/MoSe_2$ heterobilayer," Phys. Rev. X **11**, 031033 (2021).
[110]X. Wang, J. Zhu, K. L. Seyler, P. Rivera, H. Zheng, Y. Wang, M. He, T. Taniguchi, K. Watanabe, J. Yan *et al.*, "Moiré trions in $MoSe_2/WSe_2$ heterobilayers," Nat. Nanotechnol. **16**, 1208–1213 (2021).
[111]E. Liu, T. Taniguchi, K. Watanabe, N. M. Gabor, Y.-T. Cui, and C. H. Lui, "Excitonic and valley-polarization signatures of fractional correlated electronic phases in a WSe_2/WS_2 moiré superlattice," Phys. Rev. Lett. **127**, 037402 (2021).
[112]E. Liu, E. Barré, J. van Baren, M. Wilson, T. Taniguchi, K. Watanabe, Y.-T. Cui, N. M. Gabor, T. F. Heinz, Y.-C. Chang, and C. H. Lui, "Signatures of moiré trions in $WSe_2/MoSe_2$ heterobilayers," Nature **594**, 46–50 (2021).
[113]A. V. Kavokin, J. J. Baumberg, G. Malpuech, and F. P. Laussy, *Microcavities* (Oxford University Press, 2017), Vol. 21.
[114]F. Hu and Z. Fei, "Recent progress on exciton polaritons in layered transition-metal dichalcogenides," Adv. Opt. Mater. **8**, 1901003 (2020).
[115]T. Galfsky, Z. Sun, C. R. Considine, C.-T. Chou, W.-C. Ko, Y.-H. Lee, E. E. Narimanov, and V. M. Menon, "Broadband enhancement of spontaneous emission in two-dimensional semiconductors using photonic hypercrystals," Nano Lett. **16**, 4940–4945 (2016).
[116]H. H. Fang, B. Han, C. Robert, M. A. Semina, D. Lagarde, E. Courtade, T. Taniguchi, K. Watanabe, T. Amand, B. Urbaszek *et al.*, "Control of the exciton radiative lifetime in van der Waals heterostructures," Phys. Rev. Lett. **123**, 067401 (2019).
[117]Y.-C. Lee, Y.-C. Tseng, and H.-L. Chen, "Single type of nanocavity structure enhances light outcouplings from various two-dimensional materials by over 100-fold," ACS Photonics **4**, 93–105 (2017).
[118]A. Krasnok, S. Lepeshov, and A. Alú, "Nanophotonics with 2D transition metal dichalcogenides," Opt. Express **26**, 15972–15994 (2018).
[119]M. Cotrufo, L. Sun, J. Choi, A. Alù, and X. Li, "Enhancing functionalities of atomically thin semiconductors with plasmonic nanostructures," Nanophotonics **8**, 577–598 (2019).
[120]M. Bernardi, M. Palummo, and J. C. Grossman, "Extraordinary sunlight absorption and one nanometer thick photovoltaics using two-dimensional monolayer materials," Nano Lett. **13**, 3664–3670 (2013).
[121]I. Epstein, B. Terrés, A. J. Chaves, V.-V. Pusapati, D. A. Rhodes, B. Frank, V. Zimmermann, Y. Qin, K. Watanabe, T. Taniguchi *et al.*, "Near-unity light absorption in a monolayer WS_2 van der Waals heterostructure cavity," Nano Lett. **20**, 3545–3552 (2020).
[122]J. Horng, E. W. Martin, Y.-H. Chou, E. Courtade, T.-c. Chang, C.-Y. Hsu, M.-H. Wentzel, H. G. Ruth, T.-c. Lu, S. T. Cundiff *et al.*, "Perfect absorption by an atomically thin crystal," Phys. Rev. Appl. **14**, 024009 (2020).
[123]C. Schneider, M. M. Glazov, T. Korn, S. Höfling, and B. Urbaszek, "Two-dimensional semiconductors in the regime of strong light-matter coupling," Nat. Commun. **9**, 2695 (2018).
[124]L. Zhao, Q. Shang, M. Li, Y. Liang, C. Li, and Q. Zhang, "Strong exciton-photon interaction and lasing of two-dimensional transition metal dichalcogenide semiconductors," Nano Res. **14**, 1937–1954 (2021).
[125]I. A. Al-Ani, K. As' Ham, O. Klochan, H. T. Hattori, L. Huang, and A. Miroshnichenko, "Recent advances on strong light-matter coupling in atomically thin TMDC semiconductor materials," J. Opt. **24**, 053001 (2022).
[126]D. Sanvitto and S. Kéna-Cohen, "The road towards polaritonic devices," Nat. Mater. **15**, 1061–1073 (2016).
[127]X. Liu, T. Galfsky, Z. Sun, F. Xia, E.-c. Lin, Y.-H. Lee, S. Kéna-Cohen, and V. M. Menon, "Strong light–matter coupling in two-dimensional atomic crystals," Nat. Photonics **9**, 30–34 (2015).
[128]S. Brodbeck, S. De Liberato, M. Amthor, M. Klaas, M. Kamp, L. Worschech, C. Schneider, and S. Höfling, "Experimental verification of the very strong coupling regime in a GaAs quantum well microcavity," Phys. Rev. Lett. **119**, 027401 (2017).
[129]C. Anton-Solanas, M. Waldherr, M. Klaas, H. Suchomel, T. H. Harder, H. Cai, E. Sedov, S. Klembt, A. V. Kavokin, S. Tongay *et al.*, "Bosonic condensation of exciton–polaritons in an atomically thin crystal," Nat. Mater. **20**, 1233–1239 (2021).

[130]J. Zhao, R. Su, A. Fieramosca, W. Zhao, W. Du, X. Liu, C. Diederichs, D. Sanvitto, T. C. H. Liew, and Q. Xiong, "Ultralow threshold polariton condensate in a monolayer semiconductor microcavity at room temperature," Nano Lett. **21**, 3331–3339 (2021).
[131]H. Shan, L. Lackner, B. Han, E. Sedov, C. Rupprecht, H. Knopf, F. Eilenberger, J. Beierlein, N. Kunte, M. Esmann *et al.*, "Spatial coherence of room-temperature monolayer WSe_2 exciton-polaritons in a trap," Nat. Commun. **12**, 6406 (2021).
[132]L. Lackner, M. Dusel, O. A. Egorov, B. Han, H. Knopf, F. Eilenberger, S. Schröder, K. Watanabe, T. Taniguchi, S. Tongay *et al.*, "Tunable exciton-polaritons emerging from WS_2 monolayer excitons in a photonic lattice at room temperature," Nat. Commun. **12**, 4933 (2021).
[133]M. Wurdack, E. Estrecho, S. Todd, T. Yun, M. Pieczarka, S. K. Earl, J. A. Davis, C. Schneider, A. G. Truscott, and E. A. Ostrovskaya, "Motional narrowing, ballistic transport, and trapping of room-temperature exciton polaritons in an atomically-thin semiconductor," Nat. Commun. **12**, 5366 (2021).
[134]J. Zhao, A. Fieramosca, R. Bao, W. Du, K. Dini, R. Su, J. Feng, Y. Luo, D. Sanvitto, T. C. H. Liew, and Q. Xiong, "Nonlinear polariton parametric emission in an atomically thin semiconductor based microcavity," Nat. Nanotechnol. **17**, 396–402 (2022).
[135]S. Dufferwiel, S. Schwarz, F. Withers, A. A. Trichet, F. Li, M. Sich, O. Del Pozo-Zamudio, C. Clark, A. Nalitov, D. D. Solnyshkov *et al.*, "Exciton–polaritons in van der Waals heterostructures embedded in tunable microcavities," Nat. Commun. **6**, 8579 (2015).
[136]L. C. Flatten, Z. He, D. M. Coles, A. A. Trichet, A. W. Powell, R. A. Taylor, J. H. Warner, and J. M. Smith, "Room-temperature exciton-polaritons with two-dimensional WS_2," Sci. Rep. **6**, 33134 (2016).
[137]S. Wang, S. Li, T. Chervy, A. Shalabney, S. Azzini, E. Orgiu, J. A. Hutchison, C. Genet, P. Samorì, and T. W. Ebbesen, "Coherent coupling of WS_2 monolayers with metallic photonic nanostructures at room temperature," Nano Lett. **16**, 4368–4374 (2016).
[138]L. Zhang, R. Gogna, W. Burg, E. Tutuc, and H. Deng, "Photonic-crystal exciton-polaritons in monolayer semiconductors," Nat. Commun. **9**, 713 (2018).
[139]Y. Chen, S. Miao, T. Wang, D. Zhong, A. Saxena, C. Chow, J. Whitehead, D. Gerace, X. Xu, S.-F. Shi, and A. Majumdar, "Metasurface integrated monolayer exciton polariton," Nano Lett. **20**, 5292–5300 (2020).
[140]K. B. Arnardottir, I. V. Iorsh, T. C. H. Liew, and I. A. Shelykh, "Hyperbolic region in an array of quantum wires in a planar cavity," ACS Photonics **4**, 1165–1171 (2017).
[141]V. Kravtsov, E. Khestanova, F. A. Benimetskiy, T. Ivanova, A. K. Samusev, I. S. Sinev, D. Pidgayko, A. M. Mozharov, I. S. Mukhin, M. S. Lozhkin *et al.*, "Nonlinear polaritons in a monolayer semiconductor coupled to optical bound states in the continuum," Light: Sci. Appl. **9**, 56 (2020).
[142]W. Liu, Z. Ji, Y. Wang, G. Modi, M. Hwang, B. Zheng, V. J. Sorger, A. Pan, and R. Agarwal, "Generation of helical topological exciton-polaritons," Science **370**, 600–604 (2020).
[143]T. Karzig, C.-E. Bardyn, N. H. Lindner, and G. Refael, "Topological polaritons," Phys. Rev. X **5**, 031001 (2015).
[144]M. Li, I. Sinev, F. Benimetskiy, T. Ivanova, E. Khestanova, S. Kiriushechkina, A. Vakulenko, S. Guddala, M. Skolnick, V. M. Menon *et al.*, "Experimental observation of topological Z_2 exciton-polaritons in transition metal dichalcogenide monolayers," Nat. Commun. **12**, 4425 (2021).
[145]T. Ozawa, H. M. Price, A. Amo, N. Goldman, M. Hafezi, L. Lu, M. C. Rechtsman, D. Schuster, J. Simon, O. Zilberberg *et al.*, "Topological photonics," Rev. Mod. Phys. **91**, 015006 (2019).
[146]K. P. O'Donnell and X. Chen, "Temperature dependence of semiconductor band gaps," Appl. Phys. Lett. **58**, 2924–2926 (1991).
[147]X. Liu, W. Bao, Q. Li, C. Ropp, Y. Wang, and X. Zhang, "Control of coherently coupled exciton polaritons in monolayer tungsten disulphide," Phys. Rev. Lett. **119**, 027403 (2017).
[148]B. Chakraborty, J. Gu, Z. Sun, M. Khatoniar, R. Bushati, A. L. Boehmke, R. Koots, and V. M. Menon, "Control of strong light–matter interaction in monolayer WS_2 through electric field gating," Nano Lett. **18**, 6455–6460 (2018).
[149]Y.-J. Chen, J. D. Cain, T. K. Stanev, V. P. Dravid, and N. P. Stern, "Valley-polarized exciton–polaritons in a monolayer semiconductor," Nat. Photonics **11**, 431–435 (2017).
[150]Z. Sun, J. Gu, A. Ghazaryan, Z. Shotan, C. R. Considine, M. Dollar, B. Chakraborty, X. Liu, P. Ghaemi, S. Kéna-Cohen, and V. M. Menon, "Optical control of room-temperature valley polaritons," Nat. Photonics **11**, 491–496 (2017).
[151]S. Dufferwiel, T. P. Lyons, D. D. Solnyshkov, A. A. P. Trichet, F. Withers, S. Schwarz, G. Malpuech, J. M. Smith, K. S. Novoselov, M. S. Skolnick *et al.*, "Valley-addressable polaritons in atomically thin semiconductors," Nat. Photonics **11**, 497–501 (2017).
[152]S. Dufferwiel, T. P. Lyons, D. D. Solnyshkov, A. A. P. Trichet, A. Catanzaro, F. Withers, G. Malpuech, J. M. Smith, K. S. Novoselov, M. S. Skolnick *et al.*, "Valley coherent exciton-polaritons in a monolayer semiconductor," Nat. Commun. **9**, 4797 (2018).
[153]L. Qiu, C. Chakraborty, S. Dhara, and A. Vamivakas, "Room-temperature valley coherence in a polaritonic system," Nat. Commun. **10**, 1513 (2019).
[154]X. Liu, J. Yi, S. Yang, E.-C. Lin, Y.-J. Zhang, P. Zhang, J.-F. Li, Y. Wang, Y.-H. Lee, Z.-Q. Tian, and X. Zhang, "Nonlinear valley phonon scattering under the strong coupling regime," Nat. Mater. **20**, 1210–1215 (2021).
[155]M. Waldherr, N. Lundt, M. Klaas, S. Betzold, M. Wurdack, V. Baumann, E. Estrecho, A. Nalitov, E. Cherotchenko, H. Cai *et al.*, "Observation of bosonic condensation in a hybrid monolayer $MoSe_2$-GaAs microcavity," Nat. Commun. **9**, 3286 (2018).
[156]F. Barachati, A. Fieramosca, S. Hafezian, J. Gu, B. Chakraborty, D. Ballarini, L. Martinu, V. Menon, D. Sanvitto, and S. Kéna-Cohen, "Interacting polariton fluids in a monolayer of tungsten disulfide," Nat. Nanotechnol. **13**, 906–909 (2018).
[157]L. B. Tan, O. Cotlet, A. Bergschneider, R. Schmidt, P. Back, Y. Shimazaki, M. Kroner, and A. İmamoğlu, "Interacting polaron-polaritons," Phys. Rev. X **10**, 021011 (2020).
[158]J. Gu, V. Walther, L. Waldecker, D. Rhodes, A. Raja, J. C. Hone, T. F. Heinz, S. Kéna-Cohen, T. Pohl, and V. M. Menon, "Enhanced nonlinear interaction of polaritons via excitonic Rydberg states in monolayer WSe_2," Nat. Commun. **12**, 2269 (2021).
[159]N. Lundt, P. Nagler, A. Nalitov, S. Klembt, M. Wurdack, S. Stoll, T. H. Harder, S. Betzold, V. Baumann, A. V. Kavokin *et al.*, "Valley polarized relaxation and upconversion luminescence from Tamm-plasmon trion–polaritons with a $MoSe_2$ monolayer," 2D Mater. **4**, 025096 (2017).
[160]B. Lee, W. Liu, C. H. Naylor, J. Park, S. C. Malek, J. S. Berger, A. T. C. Johnson, and R. Agarwal, "Electrical tuning of exciton–plasmon polariton coupling in monolayer MoS_2 integrated with plasmonic nanoantenna lattice," Nano Lett. **17**, 4541–4547 (2017).
[161]J. Cuadra, D. G. Baranov, M. Wersäll, R. Verre, T. J. Antosiewicz, and T. Shegai, "Observation of tunable charged exciton polaritons in hybrid monolayer WS_2-plasmonic nanoantenna system," Nano Lett. **18**, 1777–1785 (2018).
[162]R. P. A. Emmanuele, M. Sich, O. Kyriienko, V. Shahnazaryan, F. Withers, A. Catanzaro, P. M. Walker, F. A. Benimetskiy, M. S. Skolnick, A. I. Tartakovskii *et al.*, "Highly nonlinear trion-polaritons in a monolayer semiconductor," Nat. Commun. **11**, 3589 (2020).
[163]L. Zhang, F. Wu, S. Hou, Z. Zhang, Y.-H. Chou, K. Watanabe, T. Taniguchi, S. R. Forrest, and H. Deng, "Van der Waals heterostructure polaritons with moiré-induced nonlinearity," Nature **591**, 61–65 (2021).
[164]E. M. Alexeev, D. A. Ruiz-Tijerina, M. Danovich, M. J. Hamer, D. J. Terry, P. K. Nayak, S. Ahn, S. Pak, J. Lee, J. I. Sohn, M. R. Molas, M. Koperski, K. Watanabe, T. Taniguchi, K. S. Novoselov, R. V. Gorbachev, H. S. Shin, V. I. Fal'ko, and A. I. Tartakovskii, "Resonantly hybridized excitons in moiré superlattices in van der Waals heterostructures," Nature **567**, 81–86 (2019).
[165]C. Schneider, K. Winkler, M. D. Fraser, M. Kamp, Y. Yamamoto, E. A. Ostrovskaya, and S. Höfling, "Exciton-polariton trapping and potential landscape engineering," Rep. Prog. Phys. **80**, 016503 (2016).
[166]J. M. Fitzgerald, J. J. P. Thompson, and E. Malic, "Twist angle tuning of moiré exciton polaritons in van der Waals heterostructures," Nano Lett. **22**, 4468–4474 (2022).
[167]H. Yu and W. Yao, "Electrically tunable topological transport of moiré polaritons," Sci. Bull. **65**, 1555–1562 (2020).
[168]A. Camacho-Guardian and N. R. Cooper, "Moiré-induced optical nonlinearities: Single-and multiphoton resonances," Phys. Rev. Lett. **128**, 207401 (2022).

[169]S. Latini, E. Ronca, U. De Giovannini, H. Hübener, and A. Rubio, "Cavity control of excitons in two-dimensional materials," Nano Lett. **19**, 3473–3479 (2019).
[170]D. Kutnyakhov, R. P. Xian, M. Dendzik, M. Heber, F. Pressacco, S. Y. Agustsson, L. Wenthaus, H. Meyer, S. Gieschen, G. Mercurio *et al.*, "Time- and momentum-resolved photoemission studies using time-of-flight momentum microscopy at a free-electron laser," Rev. Sci. Instrum. **91**, 013109 (2020).
[171]D. Christiansen, M. Selig, E. Malic, R. Ernstorfer, and A. Knorr, "Theory of exciton dynamics in time-resolved ARPES: Intra-and intervalley scattering in two-dimensional semiconductors," Phys. Rev. B **100**, 205401 (2019).
[172]M. Selig, G. Berghäuser, M. Richter, R. Bratschitsch, A. Knorr, and E. Malic, "Dark and bright exciton formation, thermalization, and photoluminescence in monolayer transition metal dichalcogenides," 2D Mater. **5**, 035017 (2018).
[173]M. K. L. Man, J. Madéo, C. Sahoo, K. Xie, M. Campbell, V. Pareek, A. Karmakar, E. L. Wong, A. Al-Mahboob, N. S. Chan *et al.*, "Experimental measurement of the intrinsic excitonic wave function," Sci. Adv. **7**, eabg0192 (2021).
[174]P. Steinleitner, P. Merkl, P. Nagler, J. Mornhinweg, C. Schüller, T. Korn, A. Chernikov, and R. Huber, "Direct observation of ultrafast exciton formation in a monolayer of WSe_2," Nano Lett. **17**, 1455–1460 (2017).
[175]G. Berghäuser, P. Steinleitner, P. Merkl, R. Huber, A. Knorr, and E. Malic, "Mapping of the dark exciton landscape in transition metal dichalcogenides," Phys. Rev. B **98**, 020301 (2018).
[176]R. Rosati, K. Wagner, S. Brem, R. Perea-Causín, E. Wietek, J. Zipfel, J. D. Ziegler, M. Selig, T. Taniguchi, K. Watanabe, A. Knorr, A. Chernikov, and E. Malic, "Temporal evolution of low-temperature phonon sidebands in transition metal dichalcogenides," ACS Photonics **7**, 2756–2764 (2020).
[177]F. Ceballos, Q. Cui, M. Z. Bellus, and H. Zhao, "Exciton formation in monolayer transition metal dichalcogenides," Nanoscale **8**, 11681–11688 (2016).
[178]T. Yu and M. W. Wu, "Valley depolarization due to intervalley and intravalley electron-hole exchange interactions in monolayer MoS_2," Phys. Rev. B **89**, 205303 (2014).
[179]C. R. Zhu, K. Zhang, M. Glazov, B. Urbaszek, T. Amand, Z. W. Ji, B. L. Liu, and X. Marie, "Exciton valley dynamics probed by kerr rotation in WSe_2 monolayers," Phys. Rev. B **90**, 161302 (2014).
[180]M. Selig, F. Katsch, R. Schmidt, S. Michaelis de Vasconcellos, R. Bratschitsch, E. Malic, and A. Knorr, "Ultrafast dynamics in monolayer transition metal dichalcogenides: Interplay of dark excitons, phonons, and intervalley exchange," Phys. Rev. Res. **1**, 022007 (2019).
[181]S. Xu, C. Si, Y. Li, B.-L. Gu, and W. Duan, "Valley depolarization dynamics in monolayer transition-metal dichalcogenides: Role of the satellite valley," Nano Lett. **21**, 1785–1791 (2021).
[182]C. Pöllmann, P. Steinleitner, U. Leierseder, P. Nagler, G. Plechinger, M. Porer, R. Bratschitsch, C. Schüller, T. Korn, and R. Huber, "Resonant internal quantum transitions and femtosecond radiative decay of excitons in monolayer WSe_2," Nat. Mater. **14**, 889–893 (2015).
[183]I. Paradisanos, G. Wang, E. M. Alexeev, A. R. Cadore, X. Marie, A. C. Ferrari, M. M. Glazov, and B. Urbaszek, "Efficient phonon cascades in WSe_2 monolayers," Nat. Commun. **12**, 538 (2021).
[184]M. Massicotte, F. Vialla, P. Schmidt, M. B. Lundeberg, S. Latini, S. Haastrup, M. Danovich, D. Davydovskaya, K. Watanabe, T. Taniguchi *et al.*, "Dissociation of two-dimensional excitons in monolayer WSe_2," Nat. Commun. **9**, 1633 (2018).
[185]R. Perea-Causín, S. Brem, and E. Malic, "Phonon-assisted exciton dissociation in transition metal dichalcogenides," Nanoscale **13**, 1884–1892 (2021).
[186]N. Kumar, Q. Cui, F. Ceballos, D. He, Y. Wang, and H. Zhao, "Exciton-exciton annihilation in $MoSe_2$ monolayers," Phys. Rev. B **89**, 125427 (2014).
[187]J. Zipfel, M. Kulig, R. Perea-Causín, S. Brem, J. D. Ziegler, R. Rosati, T. Taniguchi, K. Watanabe, M. M. Glazov, E. Malic, and A. Chernikov, "Exciton diffusion in monolayer semiconductors with suppressed disorder," Phys. Rev. B **101**, 115430 (2020).
[188]C. Robert, D. Lagarde, F. Cadiz, G. Wang, B. Lassagne, T. Amand, A. Balocchi, P. Renucci, S. Tongay, B. Urbaszek, and X. Marie, "Exciton radiative lifetime in transition metal dichalcogenide monolayers," Phys. Rev. B **93**, 205423 (2016).
[189]H. Wang, C. Zhang, W. Chan, C. Manolatou, S. Tiwari, and F. Rana, "Radiative lifetimes of excitons and trions in monolayers of the metal dichalcogenide MoS_2," Phys. Rev. B **93**, 045407 (2016).
[190]D. Sun, Y. Rao, G. A. Reider, G. Chen, Y. You, L. Brézin, A. R. Harutyunyan, and T. F. Heinz, "Observation of rapid exciton–exciton annihilation in monolayer molybdenum disulfide," Nano Lett. **14**, 5625–5629 (2014).
[191]S. Mouri, Y. Miyauchi, M. Toh, W. Zhao, G. Eda, and K. Matsuda, "Nonlinear photoluminescence in atomically thin layered WSe_2 arising from diffusion-assisted exciton-exciton annihilation," Phys. Rev. B **90**, 155449 (2014).
[192]L. Yuan and L. Huang, "Exciton dynamics and annihilation in WS_2 2D semiconductors," Nanoscale **7**, 7402–7408 (2015).
[193]B. Han, C. Robert, E. Courtade, M. Manca, S. Shree, T. Amand, P. Renucci, T. Taniguchi, K. Watanabe, X. Marie, L. E. Golub, M. M. Glazov, and B. Urbaszek, "Exciton states in monolayer $MoSe_2$ and $MoTe_2$ probed by upconversion spectroscopy," Phys. Rev. X **8**, 031073 (2018).
[194]Y. Hoshi, T. Kuroda, M. Okada, R. Moriya, S. Masubuchi, K. Watanabe, T. Taniguchi, R. Kitaura, and T. Machida, "Suppression of exciton-exciton annihilation in tungsten disulfide monolayers encapsulated by hexagonal boron nitrides," Phys. Rev. B **95**, 241403 (2017).
[195]A. J. Goodman, D.-H. Lien, G. H. Ahn, L. L. Spiegel, M. Amani, A. P. Willard, A. Javey, and W. A. Tisdale, "Substrate-dependent exciton diffusion and annihilation in chemically treated MoS_2 and WS_2," Chem. Phys. C **124**, 12175–12184 (2020).
[196]D. Erkensten, S. Brem, K. Wagner, R. Gillen, R. Perea-Causín, J. D. Ziegler, T. Taniguchi, K. Watanabe, J. Maultzsch, A. Chernikov, and E. Malic, "Dark exciton-exciton annihilation in monolayer WSe_2," Phys. Rev. B **104**, L241406 (2021).
[197]S. Z. Uddin, N. Higashitarumizu, H. Kim, J. Yi, X. Zhang, D. Chrzan, and A. Javey, "Enhanced neutral exciton diffusion in monolayer WS_2 by exciton–exciton annihilation," ACS Nano **16**, 8005–8011 (2022).
[198]M. Amani, D.-H. Lien, D. Kiriya, J. Xiao, A. Azcatl, J. Noh, S. R. Madhvapathy, R. Addou, S. Kc, M. Dubey *et al.*, "Near-unity photoluminescence quantum yield in MoS_2," Science **350**, 1065–1068 (2015).
[199]H. Wang, C. Zhang, and F. Rana, "Ultrafast dynamics of defect-assisted electron–hole recombination in monolayer MoS_2," Nano Lett. **15**, 339–345 (2015).
[200]D.-H. Lien, S. Z. Uddin, M. Yeh, M. Amani, H. Kim, J. W. Ager III, E. Yablonovitch, and A. Javey, "Electrical suppression of all nonradiative recombination pathways in monolayer semiconductors," Science **364**, 468–471 (2019).
[201]K.-Q. Lin, C. S. Ong, S. Bange, P. E. Faria Junior, B. Peng, J. D. Ziegler, J. Zipfel, C. Bäuml, N. Paradiso, K. Watanabe *et al.*, "Narrow-band high-lying excitons with negative-mass electrons in monolayer WSe_2," Nat. Commun. **12**, 5500 (2021).
[202]A. Singh, G. Moody, K. Tran, M. E. Scott, V. Overbeck, G. Berghäuser, J. Schaibley, E. J. Seifert, D. Pleskot, N. M. Gabor *et al.*, "Trion formation dynamics in monolayer transition metal dichalcogenides," Phys. Rev. B **93**, 041401 (2016).
[203]T. Godde, D. Schmidt, J. Schmutzler, M. Aßmann, J. Debus, F. Withers, E. M. Alexeev, O. Del Pozo-Zamudio, O. V. Skrypka, K. S. Novoselov *et al.*, "Exciton and trion dynamics in atomically thin $MoSe_2$ and WSe_2: Effect of localization," Phys. Rev. B **94**, 165301 (2016).
[204]G. Wang, L. Bouet, D. Lagarde, M. Vidal, A. Balocchi, T. Amand, X. Marie, and B. Urbaszek, "Valley dynamics probed through charged and neutral exciton emission in monolayer WSe_2," Phys. Rev. B **90**, 075413 (2014).
[205]A. Singh, K. Tran, M. Kolarczik, J. Seifert, Y. Wang, K. Hao, D. Pleskot, N. M. Gabor, S. Helmrich, N. Owschimikow *et al.*, "Long-lived valley polarization of intravalley trions in monolayer WSe_2," Phys. Rev. Lett. **117**, 257402 (2016).
[206]A. Esser, R. Zimmermann, and E. Runge, "Theory of trion spectra in semiconductor nanostructures," Phys. Status Solidi B **227**, 317–330 (2001).
[207]J. Zipfel, K. Wagner, M. A. Semina, J. D. Ziegler, T. Taniguchi, K. Watanabe, M. M. Glazov, and A. Chernikov, "Electron recoil effect in electrically tunable $MoSe_2$ monolayers," Phys. Rev. B **105**, 075311 (2022).
[208]J. W. Christopher, B. B. Goldberg, and A. K. Swan, "Long tailed trions in monolayer MoS_2: Temperature dependent asymmetry and resulting red-shift of trion photoluminescence spectra," Sci. Rep. **7**, 14062 (2017).
[209]R. Perea-Causin, S. Brem, and E. Malic, "Trion-phonon interaction in atomically thin semiconductors," Phys. Rev. B **106**, 115407 (2022).
[210]Y. You, X.-X. Zhang, T. C. Berkelbach, M. S. Hybertsen, D. R. Reichman, and T. F. Heinz, "Observation of biexcitons in monolayer WSe_2," Nat. Phys. **11**, 477–481 (2015).

[211]C. Jin, E. Y. Ma, O. Karni, E. C. Regan, F. Wang, and T. F. Heinz, "Ultrafast dynamics in van der Waals heterostructures," Nat. Nanotechnol. **13**, 994–1003 (2018).
[212]M. Plankl, P. E. Faria Junior, F. Mooshammer, T. Siday, M. Zizlsperger, F. Sandner, F. Schiegl, S. Maier, M. A. Huber, M. Gmitra, J. Fabian, J. L. Boland, T. L. Cocker, and R. Huber, "Subcycle contact-free nanoscopy of ultrafast interlayer transport in atomically thin heterostructures," Nat. Photonics **15**, 594–600 (2021).
[213]P. Merkl, F. Mooshammer, P. Steinleitner, A. Girnghuber, K.-Q. Lin, P. Nagler, J. Holler, C. Schüller, J. M. Lupton, T. Korn, S. Ovesen, S. Brem, E. Malic, and R. Huber, "Ultrafast transition between exciton phases in van der Waals heterostructures," Nat. Mater. **18**, 691–696 (2019).
[214]S. Ovesen, S. Brem, C. Linderälv, M. Kuisma, T. Korn, P. Erhart, M. Selig, and E. Malic, "Interlayer exciton dynamics in van der Waals heterostructures," Commun. Phys. **2**, 23 (2019).
[215]G. Meneghini, S. Brem, and E. Malic, "Ultrafast phonon-driven charge transfer in van der Waals heterostructures," Nat. Sci. e20220014 (2022).
[216]M. Massicotte, P. Schmidt, F. Vialla, K. G. Schädler, A. Reserbat-Plantey, K. Watanabe, T. Taniguchi, K. J. Tielrooij, and F. H. L. Koppens, "Picosecond photoresponse in van der Waals heterostructures," Nat. Nanotechnol. **11**, 42–46 (2016).
[217]J. He, N. Kumar, M. Z. Bellus, H.-Y. Chiu, D. He, Y. Wang, and H. Zhao, "Electron transfer and coupling in graphene–tungsten disulfide van der Waals heterostructures," Nat. Commun. **5**, 5622 (2014).
[218]L. Yuan, T.-F. Chung, A. Kuc, Y. Wan, Y. Xu, Y. P. Chen, T. Heine, and L. Huang, "Photocarrier generation from interlayer charge-transfer transitions in WS_2-graphene heterostructures," Sci. Adv. **4**, e1700324 (2018).
[219]E. Lorchat, L. E. P. López, C. Robert, D. Lagarde, G. Froehlicher, T. Taniguchi, K. Watanabe, X. Marie, and S. Berciaud, "Filtering the photoluminescence spectra of atomically thin semiconductors with graphene," Nat. Nanotechnol. **15**, 283–288 (2020).
[220]S. Aeschlimann, A. Rossi, M. Chávez-Cervantes, R. Krause, B. Arnoldi, B. Stadtmüller, M. Aeschlimann, S. Forti, F. Fabbri, C. Coletti, and I. Gierz, "Direct evidence for efficient ultrafast charge separation in epitaxial WS_2/graphene heterostructures," Sci. Adv. **6**, eaay0761 (2020).
[221]R. Krause, S. Aeschlimann, M. Chávez-Cervantes, R. Perea-Causin, S. Brem, E. Malic, S. Forti, F. Fabbri, C. Coletti, and I. Gierz, "Microscopic understanding of ultrafast charge transfer in van der Waals heterostructures," Phys. Rev. Lett. **127**, 276401 (2021).
[222]S. Fu, I. du Fossé, X. Jia, J. Xu, X. Yu, H. Zhang, W. Zheng, S. Krasel, Z. Chen, Z. M. Wang *et al.*, "Long-lived charge separation following pump-wavelength–dependent ultrafast charge transfer in graphene/WS_2 heterostructures," Sci. Adv. **7**, eabd9061 (2021).
[223]W. J. Yu, Y. Liu, H. Zhou, A. Yin, Z. Li, Y. Huang, and X. Duan, "Highly efficient gate-tunable photocurrent generation in vertical heterostructures of layered materials," Nat. Nanotechnol. **8**, 952–958 (2013).
[224]L. Britnell, R. M. Ribeiro, A. Eckmann, R. Jalil, B. D. Belle, A. Mishchenko, Y.-J. Kim, R. V. Gorbachev, T. Georgiou, S. V. Morozov *et al.*, "Strong light-matter interactions in heterostructures of atomically thin films," Science **340**, 1311–1314 (2013).
[225]P. Nagler, M. V. Ballottin, A. A. Mitioglu, F. Mooshammer, N. Paradiso, C. Strunk, R. Huber, A. Chernikov, P. C. M. Christianen, C. Schüller, and T. Korn, "Giant magnetic splitting inducing near-unity valley polarization in van der Waals heterostructures," Nat. Commun. **8**, 1551 (2017).
[226]P. Merkl, F. Mooshammer, S. Brem, A. Girnghuber, K.-Q. Lin, L. Weigl, M. Liebich, C.-K. Yong, R. Gillen, J. Maultzsch *et al.*, "Twist-tailoring Coulomb correlations in van der Waals homobilayers," Nat. Commun. **11**, 2167 (2020).
[227]J. Choi, M. Florian, A. Steinhoff, D. Erben, K. Tran, D. S. Kim, L. Sun, J. Quan, R. Claassen, S. Majumder *et al.*, "Twist angle-dependent interlayer exciton lifetimes in van der Waals heterostructures," Phys. Rev. Lett. **126**, 047401 (2021).
[228]T. Siday, F. Sandner, S. Brem, M. Zizlsperger, R. Perea-Causin, F. Schiegl, S. Nerreter, M. Plankl, P. Merkl, F. Mooshammer *et al.*, "Ultrafast nanoscopy of high-density exciton phases in WSe_2," Nano Lett. **22**, 2561–2568 (2022).
[229]Z. Wang, Y.-H. Chiu, K. Honz, K. F. Mak, and J. Shan, "Electrical tuning of interlayer exciton gases in WSe_2 bilayers," Nano Lett. **18**, 137–143 (2018).
[230]A. Steinhoff, M. Florian, M. Rösner, G. Schönhoff, T. O. Wehling, and F. Jahnke, "Exciton fission in monolayer transition metal dichalcogenide semiconductors," Nat. Commun. **8**, 1166 (2017).
[231]F. Cadiz, C. Robert, E. Courtade, M. Manca, L. Martinelli, T. Taniguchi, K. Watanabe, T. Amand, A. C. H. Rowe, D. Paget, B. Urbaszek, and X. Marie, "Exciton diffusion in WSe_2 monolayers embedded in a van der Waals heterostructure," Appl. Phys. Lett. **112**, 152106 (2018).
[232]M. Kulig, J. Zipfel, P. Nagler, S. Blanter, C. Schüller, T. Korn, N. Paradiso, M. M. Glazov, and A. Chernikov, "Exciton diffusion and halo effects in monolayer semiconductors," Phys. Rev. Lett. **120**, 207401 (2018).
[233]R. Perea-Causín, S. Brem, R. Rosati, R. Jago, M. Kulig, J. D. Ziegler, J. Zipfel, A. Chernikov, and E. Malic, "Exciton propagation and halo formation in two-dimensional materials," Nano Lett. **19**, 7317–7323 (2019).
[234]Z. Sun, A. Ciarrocchi, F. Tagarelli, J. F. Gonzalez Marin, K. Watanabe, T. Taniguchi, and A. Kis, "Excitonic transport driven by repulsive dipolar interaction in a van der Waals heterostructure," Nat. Photonics **16**, 79–85 (2022).
[235]L. Yuan, B. Zheng, J. Kunstmann, T. Brumme, A. B. Kuc, C. Ma, S. Deng, D. Blach, A. Pan, and L. Huang, "Twist-angle-dependent interlayer exciton diffusion in WS_2–WSe_2 heterobilayers," Nat. Mater. **19**, 617–623 (2020).
[236]R. Rosati, R. Schmidt, S. Brem, R. Perea-Causín, I. Niehues, J. Kern, J. A. Preuß, R. Schneider, S. Michaelis de Vasconcellos, R. Bratschitsch, and E. Malic, "Dark exciton anti-funneling in atomically thin semiconductors," Nat. Commun. **12**, 7221 (2021).
[237]S. Z. Uddin, H. Kim, M. Lorenzon, M. Yeh, D.-H. Lien, E. S. Barnard, H. Htoon, A. Weber-Bargioni, and A. Javey, "Neutral exciton diffusion in monolayer MoS_2," ACS Nano **14**, 13433–13440 (2020).
[238]R. K. Pathria, *Statistical Mechanics* (Elsevier, 2016).
[239]O. Hess and T. Kuhn, "Maxwell-Bloch equations for spatially inhomogeneous semiconductor lasers. I. Theoretical formulation," Phys. Rev. A **54**, 3347–3359 (1996).
[240]R. Rosati, R. Perea-Causín, S. Brem, and E. Malic, "Negative effective excitonic diffusion in monolayer transition metal dichalcogenides," Nanoscale **12**, 356–363 (2020).
[241]M. M. Glazov, "Quantum interference effect on exciton transport in monolayer semiconductors," Phys. Rev. Lett. **124**, 166802 (2020).
[242]K. Wagner, J. Zipfel, R. Rosati, E. Wietek, J. D. Ziegler, S. Brem, R. Perea-Causín, T. Taniguchi, K. Watanabe, M. M. Glazov, E. Malic, and A. Chernikov, "Nonclassical exciton diffusion in monolayer WSe_2," Phys. Rev. Lett. **127**, 076801 (2021).
[243]R. Rosati, K. Wagner, S. Brem, R. Perea-Causín, J. D. Ziegler, J. Zipfel, T. Taniguchi, K. Watanabe, A. Chernikov, and E. Malic, "Non-equilibrium diffusion of dark excitons in atomically thin semiconductors," Nanoscale **13**, 19966–19972 (2021).
[244]D. F. Cordovilla Leon, Z. Li, S. W. Jang, and P. B. Deotare, "Hot exciton transport in WSe_2 monolayers," Phys. Rev. B **100**, 241401 (2019).
[245]S. Park, B. Han, C. Boule, D. Paget, A. C. H. Rowe, F. Sirotti, T. Taniguchi, K. Watanabe, C. Robert, L. Lombez *et al.*, "Imaging Seebeck drift of excitons and trions in $MoSe_2$ monolayers," 2D Mater. **8**, 045014 (2021).
[246]M. M. Glazov, "Phonon wind and drag of excitons in monolayer semiconductors," Phys. Rev. B **100**, 045426 (2019).
[247]Y. Yu, Y. Yu, G. Li, A. A. Puretzky, D. B. Geohegan, and L. Cao, "Giant enhancement of exciton diffusivity in two-dimensional semiconductors," Sci. Adv. **6**, eabb4823 (2020).
[248]Y. Yu, A. W. Bataller, R. Younts, Y. Yu, G. Li, A. A. Puretzky, D. B. Geohegan, K. Gundogdu, and L. Cao, "Room-temperature electron–hole liquid in monolayer MoS_2," ACS Nano **13**, 10351–10358 (2019).
[249]Y. Fu, D. He, J. He, A. Bian, L. Zhang, S. Liu, Y. Wang, and H. Zhao, "Effect of dielectric environment on excitonic dynamics in monolayer WS_2," Adv. Mater. Interfaces **6**, 1901307 (2019).
[250]Z. Li, D. F. Cordovilla Leon, W. Lee, K. Datta, Z. Lyu, J. Hou, T. Taniguchi, K. Watanabe, E. Kioupakis, and P. B. Deotare, "Dielectric engineering for manipulating exciton transport in semiconductor monolayers," Nano Lett. **21**, 8409–8417 (2021).
[251]M. G. Harats, J. N. Kirchhof, M. Qiao, K. Greben, and K. I. Bolotin, "Dynamics and efficient conversion of excitons to trions in non-uniformly strained monolayer WS_2," Nat. Photonics **14**, 324–329 (2020).

[252]R. Rosati, S. Brem, R. Perea-Causín, R. Schmidt, I. Niehues, S. Michaelis de Vasconcellos, R. Bratschitsch, and E. Malic, "Strain-dependent exciton diffusion in transition metal dichalcogenides," 2D Mater. **8**, 015030 (2021).
[253]G. Cheng, B. Li, Z. Jin, M. Zhang, and J. Wang, "Observation of diffusion and drift of the negative trions in monolayer WS_2," Nano Lett. **21**, 6314–6320 (2021).
[254]Z. Peng, X. Chen, Y. Fan, D. J. Srolovitz, and D. Lei, "Strain engineering of 2D semiconductors and graphene: From strain fields to band-structure tuning and photonic applications," Light: Sci. Appl. **9**, 190 (2020).
[255]I. Niehues, R. Schmidt, M. Drüppel, P. Marauhn, D. Christiansen, M. Selig, G. Berghäuser, D. Wigger, R. Schneider, L. Braasch, R. Koch, A. Castellanos-Gomez, T. Kuhn, A. Knorr, E. Malic, M. Rohlfing, S. Michaelis de Vasconcellos, and R. Bratschitsch, "Strain control of exciton–phonon coupling in atomically thin semiconductors," Nano Lett. **18**, 1751–1757 (2018).
[256]A. Raja, A. Chaves, J. Yu, G. Arefe, H. M. Hill, A. F. Rigosi, T. C. Berkelbach, P. Nagler, C. Schüller, T. Korn, C. Nuckolls, J. Hone, L. E. Brus, T. F. Heinz, D. R. Reichman, and A. Chernikov, "Coulomb engineering of the bandgap and excitons in two-dimensional materials," Nat. Commun. **8**, 15251 (2017).
[257]Z. Khatibi, M. Feierabend, M. Selig, S. Brem, C. Linderälv, P. Erhart, and E. Malic, "Impact of strain on the excitonic linewidth in transition metal dichalcogenides," 2D Mater. **6**, 015015 (2018).
[258]B. Aslan, M. Deng, and T. F. Heinz, "Strain tuning of excitons in monolayer WSe_2," Phys. Rev. B **98**, 115308 (2018).
[259]M. Mrejen, L. Yadgarov, A. Levanon, and H. Suchowski, "Transient exciton-polariton dynamics in WSe_2 by ultrafast near-field imaging," Sci. Adv. **5**, eaat9618 (2019).
[260]N. Lundt, Ł. Dusanowski, E. Sedov, P. Stepanov, M. M. Glazov, S. Klembt, M. Klaas, J. Beierlein, Y. Qin, S. Tongay, M. Richard, A. V. Kavokin, S. Höfling, and C. Schneider, "Optical valley Hall effect for highly valley-coherent exciton-polaritons in an atomically thin semiconductor," Nat. Nanotechnol. **14**, 770–775 (2019).
[261]Y. Kim and J. Kim, "Near-field optical imaging and spectroscopy of 2D-TMDs," Nanophotonics **10**, 3397–3415 (2021).
[262]A. Castellanos-Gomez, R. Roldán, E. Cappelluti, M. Buscema, F. Guinea, H. S. J. van der Zant, and G. A. Steele, "Local strain engineering in atomically thin MoS_2," Nano Lett. **13**, 5361–5366 (2013).
[263]A. V. Tyurnina, D. A. Bandurin, E. Khestanova, V. G. Kravets, M. Koperski, F. Guinea, A. N. Grigorenko, A. K. Geim, and I. V. Grigorieva, "Strained bubbles in van der Waals heterostructures as local emitters of photoluminescence with adjustable wavelength," ACS Photonics **6**, 516–524 (2019).
[264]C. Carmesin, M. Lorke, M. Florian, D. Erben, A. Schulz, T. O. Wehling, and F. Jahnke, "Quantum-dot-like states in molybdenum disulfide nanostructures due to the interplay of local surface wrinkling, strain, and dielectric confinement," Nano Lett. **19**, 3182–3186 (2019).
[265]T. P. Darlington, C. Carmesin, M. Florian, E. Yanev, O. Ajayi, J. Ardelean, D. A. Rhodes, A. Ghiotto, A. Krayev, K. Watanabe, T. Taniguchi, J. W. Kysar, A. N. Pasupathy, J. C. Hone, F. Jahnke, N. J. Borys, and P. J. Schuck, "Imaging strain-localized excitons in nanoscale bubbles of monolayer WSe_2 at room temperature," Nat. Nanotechnol. **15**, 854–860 (2020).
[266]A. Branny, S. Kumar, R. Proux, and B. D. Gerardot, "Deterministic strain-induced arrays of quantum emitters in a two-dimensional semiconductor," Nat. Commun. **8**, 15053 (2017).
[267]C. Palacios-Berraquero, D. M. Kara, A. R.-P. Montblanch, M. Barbone, P. Latawiec, D. Yoon, A. K. Ott, M. Loncar, A. C. Ferrari, and M. Atatüre, "Large-scale quantum-emitter arrays in atomically thin semiconductors," Nat. Commun. **8**, 15093 (2017).
[268]J. Feng, X. Qian, C.-W. Huang, and J. Li, "Strain-engineered artificial atom as a broad-spectrum solar energy funnel," Nat. Photonics **6**, 866–872 (2012).
[269]J. Kern, I. Niehues, P. Tonndorf, R. Schmidt, D. Wigger, R. Schneider, T. Stiehm, S. Michaelis de Vasconcellos, D. E. Reiter, T. Kuhn, and R. Bratschitsch, "Nanoscale positioning of single-photon emitters in atomically thin WSe_2," Adv. Mater. **28**, 7101–7105 (2016).
[270]D. Unuchek, A. Ciarrocchi, A. Avsar, Z. Sun, K. Watanabe, T. Taniguchi, and A. Kis, "Valley-polarized exciton currents in a van der Waals heterostructure," Nat. Nanotechnol. **14**, 1104–1109 (2019).
[271]D. Erkensten, S. Brem, R. Perea-Causín, and E. Malic, "Microscopic origin of anomalous interlayer exciton transport in van der Waals heterostructures," Phys. Rev. Mater. **6**, 094006 (2022).
[272]H. Li, A. W. Contryman, X. Qian, S. M. Ardakani, Y. Gong, X. Wang, J. M. Weisse, C. H. Lee, J. Zhao, P. M. Ajayan, J. Li, H. C. Manoharan, and X. Zheng, "Optoelectronic crystal of artificial atoms in strain-textured molybdenum disulphide," Nat. Commun. **6**, 7381 (2015).
[273]D. F. Cordovilla Leon, Z. Li, S. W. Jang, C.-H. Cheng, and P. B. Deotare, "Exciton transport in strained monolayer WSe_2," Appl. Phys. Lett. **113**, 252101 (2018).
[274]H. Moon, G. Grosso, C. Chakraborty, C. Peng, T. Taniguchi, K. Watanabe, and D. Englund, "Dynamic exciton funneling by local strain control in a monolayer semiconductor," Nano Lett. **20**, 6791–6797 (2020).
[275]H. Su, D. Xu, S.-W. Cheng, B. Li, S. Liu, K. Watanabe, T. Taniguchi, T. C. Berkelbach, J. C. Hone, and M. Delor, "Dark-exciton driven energy funneling into dielectric inhomogeneities in two-dimensional semiconductors," Nano Lett. **22**, 2843–2850 (2022).
[276]R. J. Gelly, D. Renaud, X. Liao, B. Pingault, S. Bogdanovic, G. Scuri, K. Watanabe, T. Taniguchi, B. Urbaszek, H. Park, and M. Lončar, "Probing dark exciton navigation through a local strain landscape in a WSe_2 monolayer," Nat. Commun. **13**, 232 (2022).
[277]Y. Koo, Y. Kim, S. H. Choi, H. Lee, J. Choi, D. Y. Lee, M. Kang, H. S. Lee, K. K. Kim, G. Lee, and K.-D. Park, "Tip-induced nano-engineering of strain, bandgap, and exciton funneling in 2D semiconductors," Adv. Mater. **33**, 2008234 (2021).
[278]K. Datta, Z. Li, Z. Lyu, and P. B. Deotare, "Piezoelectric modulation of excitonic properties in monolayer WSe_2 under strong dielectric screening," ACS Nano **15**, 12334–12341 (2021).
[279]K. Datta, Z. Lyu, Z. Li, T. Taniguchi, K. Watanabe, and P. B. Deotare, "Spatiotemporally controlled room-temperature exciton transport under dynamic strain," Nat. Photonics **16**, 242–247 (2022).
[280]F. Dirnberger, J. D. Ziegler, P. E. Faria Junior, R. Bushati, T. Taniguchi, K. Watanabe, J. Fabian, D. Bougeard, A. Chernikov, and V. M. Menon, "Quasi-1D exciton channels in strain-engineered 2D materials," Sci. Adv. **7**, eabj3066 (2021).
[281]P. Nagler, G. Plechinger, M. V. Ballottin, A. Mitioglu, S. Meier, N. Paradiso, C. Strunk, A. Chernikov, P. C. M. Christianen, C. Schüller, and T. Korn, "Interlayer exciton dynamics in a dichalcogenide monolayer heterostructure," 2D Mater. **4**, 025112 (2017).
[282]A. L. Ivanov, "Quantum diffusion of dipole-oriented indirect excitons in coupled quantum wells," Europhys. Lett. **59**, 586 (2002).
[283]C. Schindler and R. Zimmermann, "Analysis of the exciton-exciton interaction in semiconductor quantum wells," Phys. Rev. B **78**, 045313 (2008).
[284]C. Ciuti, V. Savona, C. Piermarocchi, A. Quattropani, and P. Schwendimann, "Role of the exchange of carriers in elastic exciton-exciton scattering in quantum wells," Phys. Rev. B **58**, 7926 (1998).
[285]V. Shahnazaryan, I. Iorsh, I. A. Shelykh, and O. Kyriienko, "Exciton-exciton interaction in transition-metal dichalcogenide monolayers," Phys. Rev. B **96**, 115409 (2017).
[286]S. Ben-Tabou de-Leon and B. Laikhtman, "Exciton-exciton interactions in quantum wells: Optical properties and energy and spin relaxation," Phys. Rev. B **63**, 125306 (2001).
[287]O. Kyriienko, E. B. Magnusson, and I. A. Shelykh, "Spin dynamics of cold exciton condensates," Phys. Rev. B **86**, 115324 (2012).
[288]D. Baghdasaryan, E. Hakobyan, D. Hayrapetyan, I. Iorsh, I. Shelykh, and V. Shahnazaryan, "Tunable strongly interacting dipolar excitons in hybrid perovskites," Phys. Rev. Mater. **6**, 034003 (2022).
[289]J. Choi, W.-T. Hsu, L.-S. Lu, L. Sun, H.-Y. Cheng, M.-H. Lee, J. Quan, K. Tran, C.-Y. Wang, M. Staab *et al.*, "Moiré potential impedes interlayer exciton diffusion in van der Waals heterostructures," Sci. Adv. **6**, eaba8866 (2020).
[290]J. Wang, Q. Shi, E.-M. Shih, L. Zhou, W. Wu, Y. Bai, D. Rhodes, K. Barmak, J. Hone, C. R. Dean, and X.-Y. Zhu, "Diffusivity reveals three distinct phases of interlayer excitons in $MoSe_2/WSe_2$ heterobilayers," Phys. Rev. Lett. **126**, 106804 (2021).
[291]N. Götting, F. Lohof, and C. Gies, "Moiré-Bose-Hubbard model for interlayer excitons in twisted transition metal dichalcogenide heterostructures," Phys. Rev. B **105**, 165419 (2022).

[292]A. Julku, "Nonlocal interactions and supersolidity of moiré excitons," Phys. Rev. B **106**, 035406 (2022).
[293]X. Duan, C. Wang, J. C. Shaw, R. Cheng, Y. Chen, H. Li, X. Wu, Y. Tang, Q. Zhang, A. Pan, J. Jiang, R. Yu, Y. Huang, and X. Duan, "Lateral epitaxial growth of two-dimensional layered semiconductor heterojunctions," Nat. Nanotechnol. **9**, 1024–1030 (2014).
[294]Y. Gong, J. Lin, X. Wang, G. Shi, S. Lei, Z. Lin, X. Zou, G. Ye, R. Vajtai, B. I. Yakobson, H. Terrones, M. Terrones, B. K. Tay, J. Lou, S. T. Pantelides, Z. Liu, W. Zhou, and P. M. Ajayan, "Vertical and in-plane heterostructures from WS_2/MoS_2 monolayers," Nat. Mater. **13**, 1135–1142 (2014).
[295]C. Huang, S. Wu, A. M. Sanchez, J. J. P. Peters, R. Beanland, J. S. Ross, P. Rivera, W. Yao, D. H. Cobden, and X. Xu, "Lateral heterojunctions within monolayer $MoSe_2$–WSe_2 semiconductors," Nat. Mater. **13**, 1096–1101 (2014).
[296]M.-Y. Li, Y. Shi, C.-C. Cheng, L.-S. Lu, Y.-C. Lin, H.-L. Tang, M.-L. Tsai, C.-W. Chu, K.-H. Wei, J.-H. He, W.-H. Chang, K. Suenaga, and L.-J. Li, "Epitaxial growth of a monolayer WSe_2-MoS_2 lateral p-n junction with an atomically sharp interface," Science **349**, 524–528 (2015).
[297]H. Heo, J. H. Sung, G. Jin, J.-H. Ahn, K. Kim, M.-J. Lee, S. Cha, H. Choi, and M.-H. Jo, "2D materials: Rotation-misfit-free heteroepitaxial stacking and stitching growth of hexagonal transition-metal dichalcogenide monolayers by nucleation kinetics controls," Adv. Mater. **27**, 3839 (2015).
[298]Z. Zhang, P. Chen, X. Duan, K. Zang, J. Luo, and X. Duan, "Robust epitaxial growth of two-dimensional heterostructures, multiheterostructures, and superlattices," Science **357**, 788–792 (2017).
[299]P. K. Sahoo, S. Memaran, Y. Xin, L. Balicas, and H. R. Gutiérrez, "One-pot growth of two-dimensional lateral heterostructures via sequential edge-epitaxy," Nature **553**, 63–67 (2018).
[300]L. Yuan, B. Zheng, Q. Zhao, R. Kempt, T. Brumme, A. B. Kuc, C. Ma, S. Deng, A. Pan, and L. Huang, "Non-equilibrium first-order exciton mott transition at monolayer lateral heterojunctions visualized by ultrafast microscopy," arXiv:2111.07887 (2021).
[301]K. W. Lau, Calvin, Z. Gong, H. Yu, and W. Yao, "Interface excitons at lateral heterojunctions in monolayer semiconductors," Phys. Rev. B **98**, 115427 (2018).
[302]M. Z. Bellus, M. Mahjouri-Samani, S. D. Lane, A. D. Oyedele, X. Li, A. A. Puretzky, D. Geohegan, K. Xiao, and H. Zhao, "Photocarrier transfer across monolayer MoS_2–$MoSe_2$ lateral heterojunctions," ACS Nano **12**, 7086–7092 (2018).
[303]D. Beret, I. Paradisanos, Z. Gan, A. George, T. Lehnert, J. Biskupek, S. Shree, A. Estrada-Real, D. Lagarde, J.-M. Poumirol *et al.*, "Exciton spectroscopy and diffusion in $MoSe_2$-WSe_2 lateral heterostructures encapsulated in hexagonal boron nitride," arXiv:2204.07351 (2022).
[304]M. Shimasaki, T. Nishihara, K. Matsuda, T. Endo, Y. Takaguchi, Z. Liu, Y. Miyata, and Y. Miyauchi, "Directional exciton-energy transport in a lateral heteromonolayer of WSe_2–$MoSe_2$," ACS Nano **16**, 8205 (2022).
[305]J. Li, M. Goryca, J. Choi, X. Xu, and S. A. Crooker, "Many-body exciton and intervalley correlations in heavily electron-doped WSe_2 monolayers," Nano Lett. **22**, 426–432 (2021).
[306]D. Van Tuan, S.-F. Shi, X. Xu, S. A. Crooker, and H. Dery, "Six-body and eight-body exciton states in monolayer WSe_2," Phys. Rev. Lett. **129**, 076801 (2022).
[307]T. Smoleński, P. E. Dolgirev, C. Kuhlenkamp, A. Popert, Y. Shimazaki, P. Back, X. Lu, M. Kroner, K. Watanabe, T. Taniguchi *et al.*, "Signatures of Wigner crystal of electrons in a monolayer semiconductor," Nature **595**, 53–57 (2021).
[308]S. Brem and E. Malic, "Terahertz fingerprint of monolayer Wigner crystals," Nano Lett. **22**, 1311–1315 (2022).
[309]Y. N. Joglekar, A. V. Balatsky, and S. Das Sarma, "Wigner supersolid of excitons in electron-hole bilayers," Phys. Rev. B **74**, 233302 (2006).
[310]Y.-H. Zhang, D. N. Sheng, and A. Vishwanath, "SU(4) chiral spin liquid, exciton supersolid, and electric detection in moiré bilayers," Phys. Rev. Lett. **127**, 247701 (2021).
[311]F. Lengers, T. Kuhn, and D. E. Reiter, "Phonon signatures in spectra of exciton polaritons in transition metal dichalcogenides," Phys. Rev. B **104**, L241301 (2021).
[312]B. Ferreira, R. Rosati, and E. Malic, "Microscopic modeling of exciton-polariton diffusion coefficients in atomically thin semiconductors," Phys. Rev. Mater. **6**, 034008 (2022).
[313]D. Li, H. Shan, C. Rupprecht, H. Knopf, K. Watanabe, T. Taniguchi, Y. Qin, S. Tongay, M. Nuß, S. Schröder *et al.*, "Hybridized exciton-photon-phonon states in a transition metal dichalcogenide van der Waals heterostructure microcavity," Phys. Rev. Lett. **128**, 087401 (2022).
[314]B. Datta, M. Khatoniar, P. Deshmukh, R. Bushati, S. De Liberato, S. K. Cohen, and V. M. Menon, "Highly non-linear interlayer exciton-polaritons in bilayer MoS_2," arXiv:2110.13326 (2021).
[315]C. Louca, A. Genco, S. Chiavazzo, T. P. Lyons, S. Randerson, C. Trovatello, P. Claronino, R. Jayaprakash, K. Watanabe, T. Taniguchi, *et al.*, "Nonlinear interactions of dipolar excitons and polaritons in MoS_2 bilayers," arXiv:2204.00485 (2022).
[316]P. Cristofolini, G. Christmann, S. I. Tsintzos, G. Deligeorgis, G. Konstantinidis, Z. Hatzopoulos, P. G. Savvidis, and J. J. Baumberg, "Coupling quantum tunneling with cavity photons," Science **336**, 704–707 (2012).